Inorganic Chemistry
Article

Inorg. Chem. **2009**, *48*, 10591–10607 **10591**
DOI: 10.1021/ic901257s

Synthesis, Structures, and Properties of 1,2,4,5-Benzenetetrathiolate Linked Group 10 Metal Complexes

Kuppuswamy Arumugam,[†] Mohamed C. Shaw,[†] P. Chandrasekaran,[†] Dino Villagrán,[‡] Thomas G. Gray,[*,§] Joel T. Mague,[†] and James P. Donahue[*,†]

[†]*Department of Chemistry, Tulane University, 6400 Freret Street, New Orleans, Louisiana 70118-5698,* [‡]*Department of Chemistry, Massachusetts Institute of Technology, 77 Massachusetts Avenue, Cambridge, Massachusetts 02139, and* [§]*Department of Chemistry, Case Western Reserve University, 10900 Euclid Avenue, Cleveland, Ohio*

Received June 30, 2009

Dimetallic compounds [(P−P)M($S_2C_6H_2S_2$)M(P−P)] (M=Ni, Pd; P-P=chelating bis(phosphine), **3a**-**3f**) are prepared from O=$CS_2C_6H_2S_2C$=O or $^nBu_2SnS_2C_6H_2S_2Sn^nBu_2$, which are protected forms of 1,2,4,5-benzenetetrathiolate. Selective monodeprotections of O=$CS_2C_6H_2S_2C$=O or $^nBu_2SnS_2C_6H_2S_2Sn^nBu_2$ lead to [(P−P)Ni($S_2C_6H_2S_2C$=O)] or [(P−P)Ni($S_2C_6H_2S_2Sn^nBu_2$)]; the former is used to prepare trimetallic compounds [(dcpe)Ni($S_2C_6H_2S_2$)M($S_2C_6H_2S_2$)Ni(dcpe)] (M = Ni (**6a**) or Pt (**6b**); dcpe = 1,2-bis(dicyclohexylphosphino)ethane). Compounds **3a**-**3f** are redox active and display two oxidation processes, of which the first is generally reversible. Dinickel compound [(dcpe)Ni($S_2C_6H_2S_2$)Ni(dcpe)] (**3d**) reveals two reversible oxidation waves with $\Delta E_{1/2}$=0.66 V, corresponding to K_c of 1.6×10^{11} for the mixed valence species. Electrochemical behavior is unstable to repeated scanning in the presence of [Bu_4N][PF_6] electrolyte but indefinitely stable with Na[$BArF_{24}$] ($BArF_{24}$ = tetrakis(3,5-bis(trifluoromethyl)phenyl)borate), suggesting that the radical cation generated by oxidation is vulnerable to reaction with PF_6^-. Chemical oxidation of **3d** with [Cp_2Fe][$BArF_{24}$] leads to formation of [**3d**][$BArF_{24}$]. Structural identification of [**3d**][$BArF_{24}$] reveals appreciable shortening and lengthening of C−S and C−C bond distances, respectively, within the tetrathioarene fragment compared to charge-neutral **3d**, indicating this to be the redox active moiety. Attempted oxidation of [(dppb)Ni($S_2C_6H_2S_2$)Ni(dppb)] (**3c**) (dppb = 1,2-bis(diphenylphosphino)benzene) with $AgBArF_{24}$ produces [[(dppb)Ni($S_2C_6H_2S_2$)Ni(dppb)]$_2$(μ-Ag_2)][$BArF_{24}$]$_2$, [**4c**][$BArF_{24}$]$_2$, in which no redox chemistry has occurred. Crystal structures of bis(disulfide)-linked compounds [(P−P)Ni($S_2C_6H_2$(μ-S_2)$_2C_6H_2S_2$)Ni(P−P)] are reported. Near IR spectroscopy upon cationic [**3d**]$^+$ and neutral **6a** reveals multiple intense absorptions in the 950−1400 nm region. Time-dependent density functional theory (DFT) calculations on a **6a** model compound indicate that these absorptions are transitions between ligand-based π-type orbitals that have significant contributions from the sulfur p orbitals.

Introduction

Metallodithiolene complexes have been the subject of extensive study because of the possible applications arising from their conducting, magnetic, and optical properties. Much of this work has dealt with planar monometallic complexes of the Group 10 metals, which in the crystalline state typically form stacking arrangements that enable electronic delocalization.[1−4] More recently, a variety of dimetallic complexes with a dithiolene-type connecting ligand, most with tetrathiooxalate (tto^{2-}), have been described.[5−13] These species are still planar, or nearly so, and offer the possibility

*To whom correspondence should be addressed. E-mail: donahue@tulane.edu.

(1) Cassoux, P.; Valade, L.; Kobayashi, H.; Kobayashi, A.; Clark, R. A.; Underhill, A. E. *Coord. Chem. Rev.* **1991**, *110*, 115–160.
(2) Pullen, A. E.; Olk, R.-M. *Coord. Chem. Rev.* **1999**, *188*, 211–262.
(3) Robertson, N.; Cronin, L. *Coord. Chem. Rev.* **2002**, *227*, 93–127.
(4) Faulmann, C.; Cassoux, P. *Prog. Inorg. Chem.* **2004**, *52*, 399–489.
(5) Piotraschke, J.; Pullen, A. E.; Abboud, K. A.; Reynolds, J. R. *Inorg. Chem.* **1995**, *34*, 4011–4012.
(6) Pullen, A. E.; Zeltner, S.; Olk, R.-M.; Hoyer, E.; Abboud, K. A.; Reynolds, J. R. *Inorg. Chem.* **1996**, *35*, 4420–4426.
(7) Pullen, A. E.; Olk, R.-M.; Zeltner, S.; Hoyer, E.; Abboud, K. A.; Reynolds, J. R. *Inorg. Chem.* **1997**, *36*, 958–959.
(8) Pullen, A. E.; Zeltner, S.; Olk, R.-M.; Hoyer, E.; Abboud, K. A.; Reynolds, J. R. *Inorg. Chem.* **1997**, *36*, 4163–4171.
(9) Vicente, R.; Ribas, J.; Alvarez, S.; Segui, A.; Solans, X.; Verdaguer, M. *Inorg. Chem.* **1987**, *26*, 4004–4009.
(10) Yang, X.; Doxsee, D. D.; Rauchfuss, T. B.; Wilson, S. R. *J. Chem. Soc., Chem. Commun.* **1994**, 821–822.
(11) Batsanov, A. S.; Bryce, M. R.; Dhindsa, A. S.; Howard, J. A. K.; Underhill, A. E. *Polyhedron* **2001**, *20*, 537–540.
(12) Bai, J.-F.; Zuo, J.-L.; Shen, Z.; You, X.-Z.; Fun, H. K.; Chinnakali, K. *Inorg. Chem.* **2000**, *39*, 1322–1324.
(13) Kubo, K.; Nakao, A.; Yamamoto, H. M.; Kato, R. *J. Am. Chem. Soc.* **2006**, *128*, 12358–12359.

Published on Web 10/15/2009

of forming favorable columnar stacks with individual units that are more redox active and have greater electronic delocalization than their monometallic analogues. The procedures by which such dimetallic species have been prepared are variable and include the reaction of M^{2+} (M = Ni or Cu), tto^{2-}, and a suitable monodithiolene capping ligand or ligand precursor in a 2:1:2 ratio,[5−8] by oxidative[9−11] or reductive[12] decomposition of one of two dithiolene ligands in a metal bis(dithiolene) complex, and by mixing of a metal bis(dithiolene) anion with 1/2 equiv of tto^{2-}.[13] The last approach has also yielded two interesting examples of planar, trinickel tetrathiooxalate-linked species. Metallodithiolene polymers have also been described and generally observed to have electrical conductivities of $10^0-10^2\ \Omega^{-1}\ cm^{-1}$.[14−19] Presumably, conductivity in these materials is mediated through the covalent bonds of an extended metal dithiolene chain rather than through any stacking arrangement. Because of their insolubility, such metallodithiolene polymers are not readily subject to methods of physical characterization other than X-ray scattering and X-ray absorption.[18,19]

A relatively unexplored avenue in metallodithiolene materials research is the idea of developing a well-defined set of related, soluble, metallodithiolene oligomers of increasing complexity whose properties should trend in clear ways. For instance, the redox potentials measured in a set of metallodithiolene oligomers should converge toward a limiting value characteristic of the polymer. The rationale for this "oligomer approach" has been well articulated in the context of organic systems.[20] A methodology by which such a family of metallodithiolene oligomers might be prepared is via the monodeprotection of a doubly protected bis(dithiolene) ligand. The feasibility of this principle was demonstrated by Purrington, Bereman, and co-workers, who described the preparation of dimetallic compounds, including heterodimetallic compounds, with the butadienetetrathiolate connecting ligand.[21] We have applied this methodology to 1,3,5,7-tetrathia-*s*-indacene-2,6-dione, a dione protected form of 1,2,4,5-benzenetetrathiolate, because it is a bis(dithiolene) ligand better suited to promote electronic delocalization. Using various chelating diphosphine ligands as capping end groups to obviate uncontrolled polymer growth, we have applied this selective deprotection protocol to the preparation of dimetallic benzenetetrathiolate complexes of Ni and Pd and extended it to the deliberate synthesis of "linear" trimetallic complexes as well, including an example of a mixed-metal species. The syntheses, structures, electrochemistry, and absorption spectra of these compounds, interpreted with the aid of DFT calculations, are described herein. Selected leading results of this work have been communicated.[22]

Experimental Section

Literature procedures were employed for the syntheses of 1,2-bis(diphenylphosphino)benzene (dppb),[23] 1,3,5,7-tetrathia-*s*-indacene-2,6-dione,[24] $^nBu_2SnS_2C_6H_2S_2Sn^nBu_2$,[25] [(P-P)$NiX_2$] (P-P = 1,2-bis(diphenylphosphino)ethane, dppe; 1,2-bis(diphenylphosphino)ethylene, dppee; 1,2-bis(dicyclohexylphosphino)ethane, dcpe; X = halide),[26] [(cod)$PdCl_2$] (cod = 1,5-cyclooctadiene),[27] Na[$BArF_{24}$][28] ($BArF_{24}$ = tetrakis(3,5-bis(trifluoromethyl)phenyl)borate), Ag[$BArF_{24}$],[29] and [Cp_2Fe][$BArF_{24}$].[30] All other reagents were purchased from commercial sources and used as received (MCl_2 (M = Ni, Pd, Pt), 10% LiOMe in MeOH, 21% NaOEt in EtOH, $AgPF_6$, I_2). Solvents were either dried with a system of drying columns from the Glass Contour Company (CH_2Cl_2, *n*-pentane, hexanes, Et_2O, THF, C_6H_6, toluene) or freshly distilled according to standard procedures[31] (MeOH, CH_3CN, 1,2-dichloroethane). Silica columns were run in the open air using 60−230 μm silica (Dynamic Adsorbents). All reactions and manipulations were conducted under an atmosphere of N_2 unless indicated otherwise.

Syntheses

[(dppe)Ni($S_2C_6H_2S_2CO$)] (2a). A procedure analogous to that described for **2d** was employed on a scale of 0.100 g $OCS_2C_6H_2S_2CO$ (0.38 mmol). Compound **2a** was purified on a silica column eluted with 1:1 CH_2Cl_2/hexanes and obtained as orange-red block crystals by evaporation of the eluant. Yield: 0.145 g, 54%. R_f (9:1 CH_2Cl_2/hexanes): 0.21. ^1H NMR (δ, ppm in CD_2Cl_2): 7.75−7.80 (m, 8H, aromatic C*H*), 7.54−7.57 (m, 4H, aromatic C*H*), 7.47−7.51 (m, 8H, aromatic C*H*), 7.39 (s, 2H, aromatic C*H*), 2.40 (d, 4H, $Ph_2PCH_2CH_2PPh_2$). ^{13}C NMR (δ, ppm in CD_2Cl_2): 191.8, 150.9, 150.8, 133.7, 131.7, 129.1, 124.4, 120.7, 27.6. ^{31}P NMR (δ, ppm in CD_2Cl_2): 59.92. Absorption spectrum (CH_2Cl_2), λ_{max} in nm (ε_M): 278 (43400), 282 (43200), 344 (sh, 9640), 354 (10600), 521 (307). MS (MALDI-TOF): 710 ($M + Na^+$). HRMS (MALDI-TOF) monoisotopic *m*/*z*: 685.9672 (calcd for $C_{33}H_{26}NiOP_2S_4$ (M^+) 685.9689). Anal. Calcd for $C_{33}H_{26}NiOP_2S_4$: C, 57.65; H, 3.81; S, 18.66. Found: C, 57.47; H, 3.93; S, 21.18.

[(dppee)Ni($S_2C_6H_2S_2CO$)] (2b). A procedure analogous to that described for **2d** was employed on a scale of 0.100 g $OCS_2C_6H_2S_2CO$ (0.38 mmol). Compound **2b** was purified on a silica column eluted with 1:1 CH_2Cl_2/hexanes and obtained as red-orange block crystals by evaporation of the eluant. Yield: 0.145 g, 55%. R_f (9:1 CH_2Cl_2/hexanes): 0.26. ^1H NMR (δ, ppm in CD_2Cl_2):

(14) Poleschner, H.; John, W.; Kempe, G.; Hoyer, E.; Fanghänel, E. *Z. Chem.* **1978**, *18*, 345–346.
(15) Rivera, N. M.; Engler, E. M.; Schumaker, R. R. *J. Chem. Soc., Chem. Commun.* **1979**, 184–185.
(16) Dirk, C. W.; Bousseau, M.; Barrett, P. H.; Moraes, F.; Wudl, F.; Heeger, A. J. *Macromolecules* **1986**, *19*, 266–269.
(17) Dahm, S.; Strunz, W.; Keller, H. J.; Schweitzer, D. *Synth. Met.* **1993**, *55*−*57*, 884–889.
(18) Vogt, T.; Faulmann, C.; Soules, R.; Lecante, P.; Mosset, A.; Castan, P.; Cassoux, P.; Galy, J. *J. Am. Chem. Soc.* **1988**, *110*, 1833–1840.
(19) Jolly, C. A.; Wang, F.; Krichene, S.; Reynolds, J. R.; Cassoux, P.; Faulmann, C. *Synth. Met.* **1989**, *29*, F189–F194.
(20) *Electronic Materials: The Oligomer Approach*; Müllen, K., Wegner, G., Eds.; Wiley-VCH: Weinheim, Germany, 1998.
(21) Keefer, C. E.; Purrington, S. T.; Bereman, R. D.; Boyle, P. D. *Inorg. Chem.* **1999**, *38*, 5437–5442.
(22) Arumugam, K.; Yu, R.; Villagrán, D.; Gray, T. G.; Mague, J. T.; Donahue, J. P. *Inorg. Chem.* **2008**, *47*, 5570–5572.
(23) McFarlane, H. C. E.; McFarlane, W. *Polyhedron* **1983**, *2*, 303–304.
(24) Larsen, J.; Bechgaard, K. *J. Org. Chem.* **1987**, *52*, 3285–3288.
(25) Nomura, M.; Fourmigué, M. *Inorg. Chem.* **2008**, *47*, 1301–1312.
(26) Angulo, I. M.; Bouwman, E.; van Gorkum, R.; Lok, S. M.; Lutz, M.; Spek, A. L. *J. Mol. Catal. A: Chem.* **2003**, *202*, 97–106.
(27) Drew, D.; Doyle, J. R. *Inorg. Synth.* **1990**, *28*, 346–349.
(28) Reger, D. L.; Little, C. A.; Lamba, J. J. S.; Brown, K. J. *Inorg. Synth.* **2004**, *34*, 5–8.
(29) Buschmann, W. E.; Miller, J. S. *Inorg. Synth.* **2002**, *33*, 83–91.
(30) Chávez, I.; Alvarez-Carena, A.; Molins, E.; Roig, A.; Maniukiewicz, W.; Arancibia, A.; Arancibia, V.; Brand, H.; Manríquez, J. M. *J. Organomet. Chem.* **2000**, *601*, 126–132.
(31) Armarego, W. L. F.; Perrin, D. D. *Purification of Laboratory Chemicals*, 4th ed.; Butterworth-Heinemann: Oxford, U.K, 2000.

7.73−7.79 (m, 8H, aromatic C*H*), 7.53−7.57 (m, 4H, aromatic C*H*), 7.46−7.50 (m, 8H, aromatic C*H*), 7.43 (s, 2H, aromatic C*H*), 7.35 (dd, 2H, vinylic C*H*). ^{13}C NMR (δ, ppm in CD_2Cl_2): 133.4, 131.8, 129.2, 120.7. ^{31}P NMR (δ, ppm in CD_2Cl_2): 67.0. Absorption spectrum (CH_2Cl_2), λ_{max} in nm (ε_M): 276 (40500), 296 (34800), 334 (sh, 9990), 352 (10200), 536 (338). MS (MALDI-TOF): 708 (M + Na^+). HRMS (MALDI-TOF) monoisotopic *m*/*z*: 683.9550 (calcd for $C_{33}H_{24}NiOP_2S_4$ (M^+) 683.9532). Anal. Calcd for $C_{33}H_{24}NiOP_2S_4$: C, 57.82; H, 3.53. Found: C, 56.53; H, 3.80.

[(dppb)Ni($S_2C_6H_2S_2CO$)] (2c). A procedure analogous to that described for **2d** was employed on a scale of 0.100 g $OCS_2C_6H_2S_2CO$ (0.38 mmol). Compound **2c** was purified on a silica column eluted with a CH_2Cl_2-hexanes mixture in which the CH_2Cl_2/hexanes ratio was incrementally varied from 0.0 to 1.0 and collected as the leading fraction. Further purification by crystallization was accomplished by diffusion of hexanes vapor into a 1,2-dichloroethane solution (solvated orange plates) or by diffusion of *n*-pentane into a CH_2Cl_2 solution (unsolvated orange columns). Yield: 0.165 g, 58%. R_f (9:1 CH_2Cl_2/hexanes): 0.23; R_f (2:3 EtOAc/hexanes): 0.50. ^{1}H NMR (δ, ppm in CD_2Cl_2): 7.61−7.66 (m, 10H, aromatic C*H*); 7.46−7.50 (m, 6H, aromatic C*H*); 7.36−7.41 (m, 10H, aromatic C*H*). ^{31}P NMR (δ, ppm in $CDCl_3$): 57.82. Absorption spectrum (CH_2Cl_2), λ_{max} in nm (ε_M): 278 (47700), 292 (46400), 340 (sh, 12500), 374 (sh, 7060), 520 (640). IR (cm^{-1}, KBr): 1640 (s, C═O), 1433 (m), 1097 (s), 755 (s), 745 (m), 709 (s), 692 (s), 548 (s), 534 (s), 521 (s). MS (MALDI-TOF): 757 (M + Na^+). HRMS (MALDI-TOF) monoisotopic *m*/*z*: 733.9677 (calcd for $C_{37}H_{26}NiOP_2S_4$ (M^+) 733.9688). Anal. Calcd for [(dppb)Ni($S_2C_6H_2S_2CO$)]·1/2($ClCH_2CH_2Cl$), $C_{38}H_{28}ClOP_2S_4Ni$: C, 58.14; H, 3.60; P, 7.89. Found: C, 58.79; H, 3.71; P, 8.22.

[(dcpe)Ni($S_2C_6H_2S_2CO$)] (2d). A 100 mL Schlenk flask with stir bar was charged with 1,3,5,7-tetrathia-*s*-indacene-2,6-dione (0.250 g, 0.97 mmol), 50 mL of 1:1 THF: MeOH, and LiOMe solution (0.47 mL, 0.041 g, 1.1 mmol). The resulting mixture was stirred for 1 h, during which time the insoluble 1,3,5,7-tetrathia-*s*-indacene-2,6-dione completely dissolved in the THF-MeOH mixture. To this homogeneous mixture was then added [(dcpe)-$NiBr_2$] (0.434 g, 0.67 mmol) as a single portion under nitrogen flow. An immediate color change from pale yellow to orange-red was observed. This mixture was stirred for 12 h at 25 °C, during which time a suspension of LiBr formed in the solution. The solution was filtered via filter cannula, and the solvent was removed under reduced pressure. The red solid residue was purified on a silica column eluted with 3:7 CH_2Cl_2/hexanes and collected as the first visible fraction. Compound **2d** readily crystallized from the eluant as fine, pale orange, flat needle crystals. Yield: 0.301 g, 62%. R_f (9:1 CH_2Cl_2/hexanes): 0.45. ^{1}H NMR (δ, ppm in CD_2Cl_2): 7.53 (s, 2H, aromatic C*H*), 2.20 (d, 4H, aliphatic C*H*), 2.09 (m, 4H, aliphatic C*H*), 1.91 (d, 4H, aliphatic C*H*), 1.82 (d, 8H, aliphatic C*H*), 1.70 (d, 4H, aliphatic C*H*), 1.55−1.20 (multiple overlapped signals, 24H, aliphatic C*H*); ^{13}C NMR (δ, ppm in CD_2Cl_2): 191.0, 149.5, 123.0, 119.5, 35.1, 34.9 (d), 28.0, 27.8, 26.2 (m), 25.9, 22.0, 21.5 (d); ^{31}P NMR (δ, ppm in CD_2Cl_2) 78.94. Absorption spectrum (CH_2Cl_2), λ_{max} in nm (ε_M): 260 (33300), 286 (57000), 344 (sh, 9280), 352 (10200), 494 (660). IR (cm^{-1}, KBr): 3437 (br), 2922 (s), 2845 (m), 1635 (s, C═O), 1503 (m), 1439 (m), 1263 (m), 1087 (m). MS (MALDI-TOF): 684 (M − CO)$^+$. HRMS (MALDI-TOF) monoisotopic *m*/*z*: 710.1548 (calcd for $C_{33}H_{50}NiOP_2S_4$ (M^+) 710.1567). Anal. Calcd for $C_{33}H_{50}NiOP_2S_4$: C, 55.70; H, 7.08; S, 18.02. Found: C, 54.90; H, 6.98; S, 18.63.

[(dcpe)Pd($S_2C_6H_2S_2CO$)] (2e). A procedure analogous to that described for **2d** was followed. Compound **2e** was only identified by X-ray crystallography (see Supporting Information).

[(dppe)Ni($S_2C_6H_2S_2$)Ni(dppe)] (3a) (Rxn III, Scheme 1). A procedure analogous to that described for the preparation of **3d** by Rxn III was employed on a scale of 0.100 g of $OCS_2C_6H_2S_2CO$ (0.38 mmol), 0.76 mL of LiOMe in MeOH (0.066 g, 1.74 mmol), and 30 mL of 1:1 THF: MeOH. After 12 h of stirring at ambient temperature under N_2, a dark green precipitate was isolated by filtration and washed with 3 × 5 mL Et_2O. Yield: 0.353 g, 82%. The solubility of **3a** was too sparing to permit ^{1}H and ^{13}C NMR characterization. ^{31}P NMR (δ, ppm in CD_2Cl_2): 57.74 (s). Absorption spectrum (CH_2Cl_2), λ_{max} in nm (ε_M): 232 (59300), 266 (61000), ∼273 (sh, 58600), 300 (74300), ∼352 (sh, 17700), ∼600 (1200). MS (MALDI-TOF): 1115.8 (M^+). HRMS (MALDI-TOF) monoisotopic *m*/*z*: 1114.0450 (calcd for $C_{58}H_{50}Ni_2P_4S_4$ (M^+) 1114.0446). Anal. Calcd for $C_{58}H_{50}Ni_2P_4S_4$: C, 62.39; H, 4.51. Found: C, 59.76; H, 4.47.

[(dppe)Ni($S_2C_6H_2S_2$)Ni(dppe)] (3a) (Rxn VI, Scheme 1). A 25 mL Schlenk flask charged with a stir bar, $^nBu_2SnS_2C_6H_2S_2Sn^nBu_2$ (0.100 g, 0.15 mmol), [(dppe)-$NiCl_2$] (0.158 g, 0.339 mmol), and 1,2-dichloroethane (20 mL) was fitted to a reflux condenser leading to a Schlenk line and refluxed under N_2 for 12 h. During this time, the initial orange suspension was converted to a dark green precipitate. The mixture was cooled, and the dark precipitate was collected by filtration, washed with 3 × 5 mL MeOH, followed by 3 × 5 mL of Et_2O, and dried under vacuum. Yield: 0.136 g, 81%.

[(dppee)Ni($S_2C_6H_2S_2$)Ni(dppee)] (3b) (Rxn VI, Scheme 1). The same procedure and scale as described in the preceding paragraph for the synthesis of **3a** by Rxn VI were employed. Yield: 0.140 g, 84%. The solubility of **3b** was too sparing to permit ^{1}H and ^{13}C NMR characterization. ^{31}P NMR (δ, ppm in CD_2Cl_2): 65.51 (s). Absorption spectrum (CH_2Cl_2), λ_{max} in nm (ε_M): 234 (70800), 270 (51200), 276 (51400), 302 (58000), ∼363 (sh, 15000), ∼621 (∼1220). MS (MALDI-TOF): 1111.8 (M^+). HRMS (MALDI-TOF) monoisotopic *m*/*z*: 1110.0159 (calcd for $C_{58}H_{46}Ni_2P_4S_4$ (M^+) 1110.0134). Anal. Calcd for $C_{58}H_{46}Ni_2P_4S_4$: C, 62.62; H, 4.17. Found: C, 61.15; H, 4.08.

[(dppb)Ni($S_2C_6H_2S_2$)Ni(dppb)] (3c) (Rxn VI, Scheme 1). The same procedure and scale as described in the preceding paragraphs for the synthesis of **3a** and **3b** by Rxn VI were employed. Yield: 0.145 g, 80%. ^{31}P NMR (δ, ppm in CD_2Cl_2): 57.14 (s). Absorption spectrum (CH_2Cl_2), λ_{max} in nm (ε_M): 232 (60500), 270 (sh, 39000), 278 (39400), 310 (51500), 408 (7880), 610 (∼1340). MS (MALDI-TOF): 1212.0 (M^+). HRMS (MALDI-TOF) monoisotopic *m*/*z*: 1210.0441 (calcd for $C_{66}H_{50}Ni_2P_4S_4$ (M^+) 1210.0447).

Scheme 1. Summary of Syntheses Reported and Definition of Numbering System by Which the Compounds Are Identified

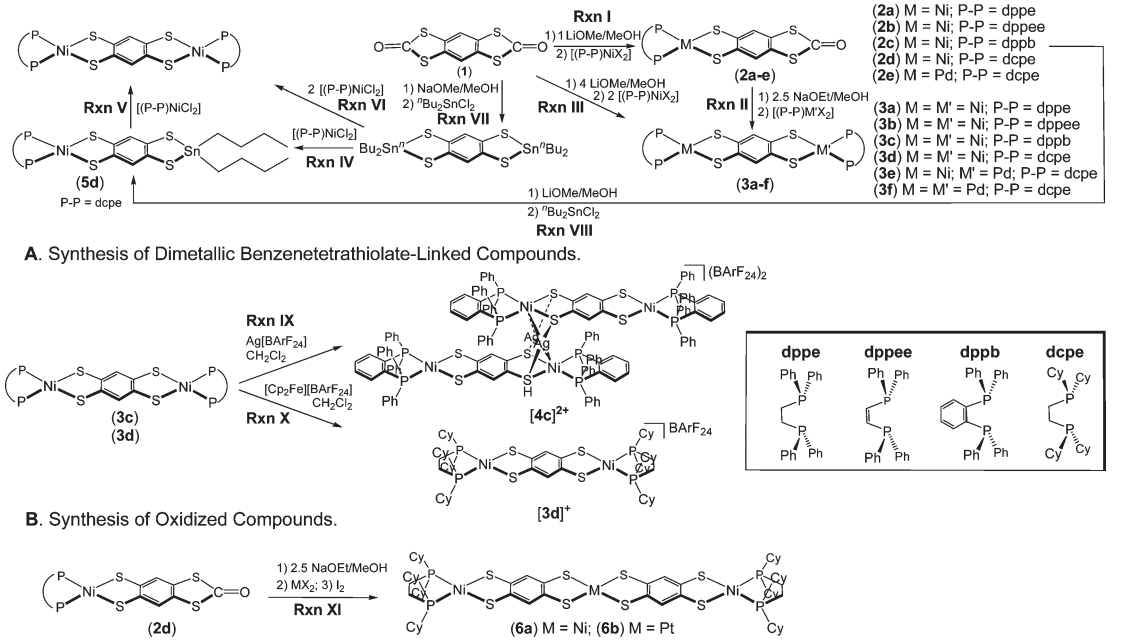

[(dcpe)Ni($S_2C_6H_2S_2$)Ni(dcpe)] (3d) (Rxn III, Scheme 1). A 50 mL Schlenk flask with stir bar was charged with 1,3,5,7-tetrathia-*s*-indacene-2,6-dione (0.079 g, 0.31 mmol), LiOMe, (0.54 mL, 0.047 g, 1.2 mmol) and 40 mL of dry 1:1 THF/MeOH. The resulting mixture was stirred under N_2 for 1 h, during which time the insoluble 1,2,5,7-tetrathia-*s*-indacene-2,6-dione completely dissolved. To the resulting mixture was added [(dcpe)$NiBr_2$] (0.353 g, 0.55 mmol) all at once as a solid under N_2 flow. An immediate change in the solution color from pale yellow to dark red was observed. This reaction mixture was stirred for 12 h at ambient temperature. This mixture was filtered via filter cannula to remove suspended LiBr, and the solvent was removed under reduced pressure. The resulting dark red solid residue was purified on a silica column eluted with a mixture of CH_2Cl_2/hexanes in which the CH_2Cl_2/hexanes ratio was incrementally varied from 0.0 to 1.0. Elution was continued with EtOAc/CH_2Cl_2 mixtures in which the EtOAc/CH_2Cl_2 ratio was similarly varied. The title compound, [(dcpe)Ni($S_2C_6H_2S_2$)Ni(dcpe)], readily crystallized from the eluant as fine, dark red plate crystals. Yield: 0.232 g, 72%. R_f (CH_2Cl_2): 0.13 (with trailing). ^{1}H NMR (δ, ppm in CD_2Cl_2): 7.35 (br s, 2H, aromatic C*H*), 2.26 (d, 8H, aliphatic C*H*), 2.08 (m, 8H, aliphatic C*H*), 1.86−1.79 (m, 32H, aliphatic C*H*), 1.69 (d, 8H, aliphatic C*H*), 1.56−1.21 (multiple overlapped signals, 40H, aliphatic C*H*). ^{13}C NMR (δ, ppm in CD_2Cl_2): 36.2, 29.5, 29.2, 27.6, 27.5, 26.6, 23.2 (t). ^{31}P NMR (δ, ppm in CD_2Cl_2): 77.23. Absorption spectrum (CH_2Cl_2), λ_{max} in nm (ε_M): 256 (44000), 296 (83400), 360 (sh, 21000), 366 (22300), 546 (970). MS (MALDI-TOF): 1164 (M^+). HRMS (MALDI-TOF) monoisotopic *m*/*z*: 1162.4226 (calcd for $C_{58}H_{98}Ni_2P_4S_4$ (M^+) 1162.4203). Anal. Calcd for $C_{58}H_{98}Ni_2P_4S_4$: C, 59.80; H, 8.48; S, 11.01. Found: C, 59.26; H, 8.68; S, 11.20.

[(dcpe)Ni($S_2C_6H_2S_2$)Ni(dcpe)] (3d) (Rxn II, Scheme 1). A 25 mL Schlenk flask with stir bar was charged with [(dcpe)Ni($S_2C_6H_2S_2$CO)] (0.050 g, 0.07 mmol), NaOEt (0.012 g, 0.176 mmol), and 20 mL of dry 1:1 THF/EtOH. The resulting mixture was stirred for 1 h, during which time the pale orange solution turned dark red in color. To this solution mixture was added [(dcpe)$NiBr_2$] (0.045 g, 0.07 mmol) as a single portion under N_2 flow, which occasioned an immediate change in the solution color from dark red to dark brown. The reaction mixture was stirred for 12 h at ambient temperature and then filtered to remove suspended LiBr. The solvent was removed from the filtrate under reduced pressure. The resulting dark red solid residue was purified as described in the preceding paragraph. Yield: 0.040 g, 49%.

[(dcpe)$PdCl_2$]. A 50 mL Schlenk flask was charged with a stir bar, 1,2-bis(dicyclohexylphosphino)ethane (dcpe) (0.226 g, 0.535 mmol) and 10 mL of dry CH_2Cl_2. A solution of [(cod)$PdCl_2$] (0.153 g, 0.536 mmol) in 20 mL of CH_2Cl_2 was slowly transferred to the dcpe solution via cannula with constant stirring. The resulting pale yellow reaction mixture was stirred at ambient temperature for 4 h. The solvent was removed under reduced pressure, and the pale yellow solid residue was washed with 2 × 10 mL of pentane and dried under vacuum for a day. Yield: 0.296 g, 92%.

[(dcpe)Ni($S_2C_6H_2S_2$)Pd(dcpe)] (3e) (Rxn II, Scheme 1). A 25 mL Schlenk flask with stir bar was charged with [(dcpe)Ni($S_2C_6H_2S_2$CO)] (0.050 g, 0.07 mmol), NaOEt, (0.012 g, 0.18 mmol), and 20 mL of dry 1:1 THF/EtOH. The resulting mixture was stirred for 1 h, during which time the pale orange solution became dark red in color. To this reaction mixture was added solid [(dcpe)$PdCl_2$] (0.042 g, 0.07 mmol) in one portion under N_2 flow, which induced an immediate change in the solution color from a dark red to a dark brown. The flask contents were stirred for 12 h at ambient temperature, during which time the formation of a NaCl suspension was noted. The reaction solution was filtered, and the solvent was removed from the filtrate under reduced pressure. The resulting dark red

solid residue was purified on a silica column eluted with a CH_2Cl_2/hexanes mixture, followed by a CH_2Cl_2/EtOAc mixture, as described for **3d**. Heterodimetallic [(dcpe)-Ni($S_2C_6H_2S_2$)Pd(dcpe)] readily crystallized from the eluant as fine, dark red crystals. Yield: 0.040 g, 47%. R_f (CH_2Cl_2): 0.14 (with trailing). ^{1}H NMR (δ, ppm in CD_2Cl_2): 7.25 (br s, 2H, aromatic C*H*), 2.25 (d, 4H, aliphatic C*H*), 2.10 (m, 12H, aliphatic C*H*), 1.97 (d, 4H, aliphatic C*H*), 1.86−1.79 (m, 24H, aliphatic C*H*), 1.68 (d, 8H, aliphatic C*H*), 1.57−1.21 (multiple overlapped signals, 44H, aliphatic C*H*). ^{13}C NMR (δ, ppm in CD_2Cl_2): 110.2, 36.5 (m), 29.5, 29.2, 29.1, 27.6 (m), 27.3 (m), 26.6, 26.4, 23.7 (t), 23.2 (t). ^{31}P NMR (δ, ppm in CD_2Cl_2): 78.32, 76.88. Absorption spectrum (CH_2Cl_2), λ_{max} in nm (ε_M): 284 (69800), 354 (sh, 15200), 364 (17600), 514 (830). MS (MALDI-TOF): 1212 (M^+).

[(dcpe)Pd($S_2C_6H_2S_2$)Pd(dcpe)] (3f) (Rxn VI, Scheme 1). A procedure similar to that described for the synthesis of **3a** by Rxn VI was used but on a scale employing 0.055 g (0.082 mmol) of $^nBu_2SnS_2C_6H_2S_2Sn^nBu_2$ and with [(dcpe)$PdCl_2$] (0.100 g, 0.167 mmol) and CH_2Cl_2 (25 mL) used in place of [(dppe)$NiCl_2$] and 1,2-dichloroethane, respectively. This reaction mixture was heated to 50 °C for 3 h, cooled to room temperature, and taken to dryness under reduced pressure. The residual solid was washed with MeOH (3 × 10 mL) and Et_2O (3 × 10 mL) and then dried under vacuum for 24 h. Compound **3f** was obtained as a brown solid and recrystallized as orange blocks by diffusion of pentane vapor into a 1,2-dichloroethane solution. Yield 0.043 g, 41%. ^{1}H NMR (δ, ppm in CD_2Cl_2): 7.18 (s, 2H, aromatic C*H*), 2.12 (br, 16H, aliphatic C*H*), 1.97 (m, 8H, aliphatic C*H*), 1.82 (br, ∼20H, aliphatic C*H*), 1.68 (m, 8H, aliphatic C*H*), 1.55 (d, ∼8H, aliphatic C*H*), 1.51 (m, ∼12H, aliphatic C*H*), 1.36−1.22 (m, 24H, aliphatic C*H*). ^{31}P NMR (δ, ppm in CD_2Cl_2): 76.78. Absorption spectrum (CH_2Cl_2), λ_{max} in nm (ε_M): 278 (109000), 350 (sh, 26300), 362 (28300). MS (MALDI-TOF): 1260 (M^+).

[(dcpe)Ni($S_2C_6H_2S_2$)Ni(dcpe)][$BArF_{24}$], [3d][$BArF_{24}$]. A 25 mL Schlenk flask with stir bar was charged with [(dcpe)Ni($S_2C_6H_2S_2$)Ni(dcpe)] (0.050 g, 0.043 mmol), [Cp_2Fe][$BArF_{24}$] (0.045 g, 0.043 mmol), and 10 mL of dry THF at 25 °C. This mixture was stirred at 25 °C for 12 h and then was taken to dryness under reduced pressure. The resulting solid residue was washed with copious amounts of hexanes and then extracted with 2 × 5 mL portions of THF. These THF extracts were filtered through Celite and taken to dryness under reduced pressure to yield [(dcpe)Ni($S_2C_6H_2S_2$)Ni(dcpe)][$BArF_{24}$]. Yield: 0.061 g, 70%. Absorption spectrum (CH_2Cl_2), λ_{max} in nm: ∼319 (sh), ∼ 386 (sh), 542 (max), ∼610 (sh), ∼680 (sh), ∼980 (sh), 1127 (max).

[[(dppb)Ni($S_2C_6H_2S_2$)Ni(dppb)]$_2$(μ-Ag_2)][$BArF_{24}$]$_2$, [4c]-[$BArF_{24}$]$_2$. A 25 mL Schlenk flask with stir bar was charged with [(dppb)Ni($S_2C_6H_2S_2$)Ni(dppb)] (0.050 g, 0.041 mmol), $AgBArF_{24}$ (0.040 g, 0.041 mmol), and 10 mL of dry CH_2Cl_2 at 25 °C. This mixture was stirred at 25 °C for 12 h, by the end of which time the insoluble [(dppb)Ni($S_2C_6H_2S_2$)Ni(dppb)] completely went into solution with an attendant change in color from green to dark red. The homogeneous reaction solution was taken to dryness under reduced pressure, and the resulting solid residue was washed with copious amounts of hexanes. The solid residue was extracted with 2 × 5 mL portions of THF, and the extracts were filtered through Celite. The solvent was removed from the filtrate under reduced pressure to yield [[(dppb)Ni($S_2C_6H_2S_2$)Ni(dppb)]$_2$-(μ-Ag_2)][$BArF_{24}$]$_2$. Yield: 0.140 g, 78%. ^{31}P NMR (δ, ppm in CD_2Cl_2): 60.70 (s), 57.84 (s). Absorption spectrum (CH_2Cl_2), λ_{max} in nm (ε_M): 261 (80000), 297 (130000), 353 (29000), 489 (3000).

[(dcpe)Ni($S_2C_6H_2S_2Sn^nBu_2$)], 5d. A 200 mL Schlenk flask with stir bar was charged with $^nBu_2SnS_2C_6H_2S_2Sn^nBu_2$ (0.286 g, 0.428 mmol) and 100 mL of dry CH_2Cl_2 at 25 °C. To a separate 100 mL Schlenk flask containing [(dcpe)$NiCl_2$] (0.250 g, 0.453 mmol) under N_2 was added 50 mL of dry CH_2Cl_2. The latter solution was added to the former solution via syringe pump at a rate of 5 mL/h over period of 10 h, during which time the slightly yellow colored solution slowly assumed an orangish hue. After the addition was complete, the resulting mixture was allowed to stir for a further 2 h at 25 °C and then was taken to dryness under reduced pressure. The dark red residue was further purified by flash chromatography on a silica column eluted with 4:6 CH_2Cl_2/hexanes to yield [(dcpe)Ni$S_2C_6H_2S_2Sn^nBu_2$]. Prolonged exposure on the silica column leads to decomposition. Yield: 0.141 g, 36%. R_f (4:6 CH_2Cl_2/hexanes): 0.27. ^{1}H NMR (δ, ppm in CD_2Cl_2): 7.42 (s, 2H, aromatic C*H*), 2.20 (d, 4H, aliphatic C*H*), 2.10 (br, 4H, aliphatic C*H*), 1.89−1.78 (m, 14H, aliphatic C*H*), 1.69 (d, 6H, aliphatic C*H*), 1.60−1.26 (multiple overlapped signals, 32H, aliphatic C*H*), 0.90 (t, 6H, −CH_3). ^{13}C NMR (δ, ppm in CD_2Cl_2): 130.0, 127.2, 36.1 (t), 29.2, 29.0, 28.1, 27.2, 26.8, 26.2, 23.0, 21.3, 13.5. ^{31}P NMR (δ, ppm in CD_2Cl_2): 78.47. Absorption spectrum (CH_2Cl_2), λ_{max} in nm (ε_M): 262 (30800), 292 (54700), 346 (8110), 358 (8060), ∼534. HRMS (MALDI-TOF) monoisotopic *m*/*z*: 912.2055 (calcd for $C_{40}H_{68}NiPS_4Sn$ (M^+) 912.2043). Anal. Calcd for $C_{40}H_{68}NiP_2S_4Sn$: C, 52.42; H, 7.48; P, 6.76. Found: C, 52.61; H, 7.29; P, 6.83.

[(dcpe)Ni($S_2C_6H_2S_2$)Ni($S_2C_6H_2S_2$)Ni(dcpe)], (6a). A 50 mL Schlenk flask with stir bar was charged with [(dcpe)Ni($S_2C_6H_2S_2CO$)] (0.200 g, 0.28 mmol), NaOEt (0.0478 g, 0.70 mmol), and dry THF/EtOH (20/20 mL). The resulting mixture was stirred under N_2 for 1 h, during which time the pale orange solution assumed a dark red color. To this reaction mixture was added solid $NiBr_2$ (0.031 g, 0.14 mmol) all at once under an outward flow of N_2. An immediate change in solution color from dark red to dark brown was observed. This mixture was stirred for 12 h at ambient temperature. After removal of the solvent under reduced pressure, the solid residue was extracted with dry CH_3CN, and the extracts were filtered through a paper filter cannula to remove the NaBr byproduct. Solid I_2 (0.071 g, 0.28 mmol) was added to the CH_3CN filtrate, which induced the formation of a brown precipitate. This heterogeneous mixture was further stirred for 2 h. The brown precipitate was isolated from the solution by filtration and dried under reduced pressure. Yield: 0.075 g, 37%. ^{31}P NMR (δ, ppm in $(CD_3)_2NC(O)D$): 79.74. Absorption spectrum (DMF), λ_{max} in nm (ε_M): 526 (1700), 689 (870), 1159 (16000), ∼1408 (9700). MS (MALDI-TOF): 1426 (M^+). HRMS (MALDI-TOF) monoisotopic *m*/*z*: 1422.2581 (calcd for $C_{64}H_{100}Ni_3P_4S_8$ (M^+) 1422.2595). Anal. Calcd for

[(dcpe)Ni($S_2C_6H_2S_2$)Ni($S_2C_6H_2S_2$)Ni(dcpe)]·2DMF, $C_{70}H_{114}N_2Ni_3O_2P_4S_8$: C, 53.48; H, 7.31; N, 1.78. Found: C, 50.46; H, 6.86, N, 1.44.

[(dcpe)Ni($S_2C_6H_2S_2$)Pt($S_2C_6H_2S_2$)Ni(dcpe)] (6b). A procedure analogous to that used for the synthesis of compound **6a** above was followed but with $PtCl_2$ used in place of $NiBr_2$. The reaction scale employed 0.150 g (0.210 mmol) of [(dcpe)Ni($S_2C_6H_2S_2CO$)], 0.028 g (0.105 mmol) of $PtCl_2$, and 0.027 g (0.106 mmol) of I_2. Yield: 0.071 g, 43%. ^{31}P NMR (ppm in $(CD_3)_2NC(O)D$): 79.22. Absorption spectrum (DMF), λ_{max} in nm (ε_M): 507 (560), 1177 (12400). MS (MALDI-TOF): 1562 (M^+).

[(dppb)Ni($S_2C_6H_2(S-S)_2C_6H_2S_2$)Ni(dppb)] 7c, [(dcpe)Ni($S_2C_6H_2(S-S)_2C_6H_2S_2$)Ni(dcpe)] 7d. Compounds **7c** and **7d** were obtained in trace amounts as adventitious byproducts attending the syntheses of compound **3c** and **3d**, respectively, and were only identified by X-ray crystallography. Deliberate, optimized preparations for **7c** and **7d** were not obtained.

Physical Methods and Calculations

UV−vis spectra (molar absorptivities reported in M^{-1} cm^{-1}) were obtained at ambient temperature with a Hewlett-Packard 8452A diode array spectrometer, while IR spectra were taken as pressed KBr pellets with a Thermo Nicolet Nexus 670 FTIR instrument in absorption mode. All NMR spectra were recorded at 25 °C either with a Varian Unity Inova spectrometer operating at 400, 100.5, and 161.8 MHz for ^{1}H, ^{13}C, and ^{31}P, respectively, or with a Bruker AVANCE 300 spectrometer operating at 121.5 MHz for ^{31}P. Spectra were referenced to the solvent residual for ^{1}H and ^{13}C and to external 85% H_3PO_4 for ^{31}P. Mass spectra (MALDI-TOF) were obtained with either an ABI Voyager-DE STR instrument or a Bruker Autoflex III instrument. Electrochemical measurements were made with a CHI620C electroanalyzer workstation using a Ag/AgCl reference electrode, a platinum disk working electrode, Pt wire as auxiliary electrode, and Bu_4NPF_6 or Na[$BArF_{24}$] as the supporting electrolyte. The Cp_2Fe^+/Cp_2Fe couple occurred at +0.54 mV (by CV) in 0.10 M [Bu_4N][PF_6] in CH_2Cl_2, at +0.30 V (by CV) in 0.01 M Na[$BArF_{24}$] in 5:4:1 CH_2Cl_2/anisole/THF, and at +0.20 V (by DPV) in 0.01 M Na[$BArF_{24}$] in CH_2Cl_2. Elemental analyses were performed by Canadian Microanalytical of Delta, British Columbia or by Midwest Microlab, LLC of Indianapolis, IN. All details regarding crystal growth, X-ray diffraction data collection, crystal structure solution and refinement, and computational work are deferred to the Supporting Information.

Results and Discussion

Syntheses. The 1,2,4,5-benzenetetrathiolate bis(dithiolene) ligand, like tto^{2-}, is expected to support extended, delocalized electronic structures in its metallocomplexes. Although polymeric $[Ni(S_2C_6H_2S_2)]_x$ was prepared and studied in 1986,[16] the first well-defined dimetal complexes with the 1,2,4,5-benzenetetrathiolate connecting ligand were $L_2M(S_2C_6H_2S_2)ML_2$ (L = Cp or η^5-$C_5H_4(SiMe_3)$; M = Ti; Zr or Hf), described by Köpf and co-workers,[32] and [(triphos)Co($S_2C_6H_2S_2$)Co(triphos)]$^{2+}$ (triphos = 1,1,1-tris(diphenylphosphanomethyl)ethane), reported by Huttner et al.[33] The arene tetrathiolate-linked anions $[[(Cl_4C_6S_2)Ni]_2(S_2C_6X_2S_2)]^{2-}$ (X = H, F, Cl), $[(F_4C_6S_2)Ni((S_2C_6F_2S_2)Ni)_n(S_2C_6F_4)]^{(n+1)-}$ (n = 4 or 5) and $[(Cl_4C_6S_2)Ni((S_2C_6Cl_2S_2)Ni)_8(S_2C_6Cl_4)]^{10-}$ have been characterized by UV−vis−near IR spectroscopy, but the samples employed in this study apparently consist of mixtures of species related by dynamic solution equilibrium processes.[34] More recently, Nomura and Fourmigué have described the synthesis and properties of Cp*Co($S_2C_6H_2S_2$)CoCp*.[25]

Preparations of benzenetetrathiol/thiolate were first reported by Testaferri and Wudl,[35,36] but a later, more facile procedure described by Bechgaard[24] has made this ligand more accessible. Because 1,2,4,5-benzenetetrathiolate is inherently very electron rich and prone to aerial oxidation, its most convenient form for handling and storage is the air-stable bis(1,3-dithiol-2-one) form, 1,3,5,7-tetrathia-*s*-indacene-2,6-dione, **1** (Scheme 1). From thence, base hydrolysis (LiOMe or NaOEt) in THF/MeOH mixtures readily liberates one or both of the ene-1,2-dithiolate moieties. Monodeprotection of this compound appears to be optimized relative to full deprotection when a substoichiometric 1 equiv of alkoxide is used.

The introduction of in situ generated $Li_2[S_2C_6H_2S_2C{=}O]$ to 1 equiv of [(P-P)MX_2] (M = Ni, Pd; X = halide; P-P = 1,2-bis(diphenylphosphino)ethane, dppe; 1,2-bis(diphenylphosphino)ethylene, dppee; 1,2-bis(diphenylphosphino)benzene, dppb; 1,2-bis(dicyclohexylphosphino)ethane, dcpe) leads to formation of the corresponding mononickel and monopalladium bis(phosphine) dithiolene compounds, [(P-P)M($S_2C_6H_2S_2C{=}O$)] (**2a**−**2e**), through halide displacement reactions (Rxn I, Scheme 1). These compounds are generally air-stable, readily soluble in polar organic solvents, and easily purified by column chromatography on silica. The immediate purpose served by the chelating bis(phosphine) ligand is prevention of the formation of undesired metal dithiolene polymer. However, since the identity of the phosphine substituents and the nature of the chelate backbone could modulate the solubility, redox potentials, and so forth of the metal complexes that are formed,[37] a variety of chelating bis(phosphines) have been studied for effect. Nickel dithiolene bis(phosphine) complexes were first prepared by Schrauzer.[38] A variety of additional examples have appeared since then, the most significant corpus of work being that contributed by Bowmaker and co-workers.[39−41]

(32) (a) Köpf, H.; Balz, H. *J. Organomet. Chem.* **1990**, *387*, 77–81. (b) Balz, H; Köpf, H.; Pickardt, J. *J. Organomet. Chem.* **1991**, *417*, 397–406.

(33) Heinze, K.; Huttner, G.; Zsolnai, L. *Z. Naturforsch., B: Chem. Sci.* **1999**, *54*, 1147–1154.

(34) Campbell, J.; Jackson, D. A.; Stark, W. M.; Watson, A. A. *Dyes Pigm.* **1991**, *15*, 15–22.

(35) Maiolo, F.; Testaferri, L.; Tiecco, M.; Tingoli, M. *J. Org. Chem.* **1981**, *46*, 3070–3073.

(36) Dirk, C. W.; Cox, S. D.; Wellman, D. E.; Wudl, F. *J. Org. Chem.* **1985**, *50*, 2395–2397.

(37) Lobana, T. S.; Gratzel, M.; Nazeeruddin, M. K.; Vlachopolous, N. *Trans. Met. Chem.* **1996**, *21*, 551–552.

(38) Mayweg, V. P.; Schrauzer, G. N. *Chem. Commun.* **1966**, 640–641.

(39) Bowmaker, G. A.; Boyd, P. D. W.; Campbell, G. K. *Inorg. Chem.* **1982**, *21*, 2403–2412.

(40) Bowmaker, G. A.; Boyd, P. D. W.; Campbell, G. K. *Inorg. Chem.* **1983**, *22*, 1208–1213.

(41) Bowmaker, G. A.; Williams, J. P. *J. Chem. Soc., Dalton Trans.* **1993**, 3593–3600.

The dinickel compounds, **3a**-**3d**, are readily prepared either by full deprotection of 1,3,5,7-tetrathia-*s*-indacene-2,6-dione (Rxn III, Scheme 1), followed by addition of 2 eq $[(P-P)NiX_2]$ (X = halide), or by starting with isolated samples of the corresponding compound **2**, deprotecting the peripheral 1,3-dithiol-2-one group, and then adding a second equiv of $[(P-P)NiX_2]$, (Rxn II, Scheme 1). Yet another way to prepare compounds **3** proceeds through di-*n*-butyl tin protected forms of benzenetetrathiolate (Rxns V and VI, Scheme 1), the doubly protected version of which was recently described by Nomura and Fourmigué.[25] A set of reactions analogous to I−III in Scheme 1, but using instead di-*n*-butyl tin as protecting group for the dithiolene chelate, can be applied for the synthesis of dinickel compounds **3** (Reactions IV−VI, respectively). Tin dithiolene compounds have been employed by others in transmetalation reactions[42,43] but have underappreciated utility for the preparation of metallodithiolene compounds. In general, the reactions which make use of the di-*n*-butyl tin protected ligand in Scheme 1 are cleaner and produce better yields than those involving the base hydrolysis of 1,3-dithiol-2-ones.

Use of isolated mononickel compounds **2a**-**2d** or **5d** affords the possibility of preparing asymmetric dimetal complexes by introduction of a $[(P-P)MX_2]$ compound differing in the identity of M and/or the chelating diphosphine. Thus, for example, the mixed nickel−palladium complex **3e** was synthesized by Rxn II. For reference purposes, dipalladium compound **3f** was also prepared by Rxn VI. The mixed metal composition of **3e** was shown not only by a MALDI-TOF mass spectrum displaying the parent ion peak, with correct isotopic distribution profile, but also by the observation of more complex NMR spectra that reflect the two distinct halves of the molecule. Compounds **3** are air-stable in the solid form but, as might be anticipated from their higher symmetry, suffer the limitation of much diminished solubility in common organic solvents. The closest analogues to compounds **3** that have been prepared are the butadienetetrathiolate-linked compound $[(dppe)Ni(S_2C_2(H)\text{-}(H)C_2S_2)Ni(dppe)]$ reported by Purrington and Bereman[21] and $[(Ph_3P)_2Pt\text{-}(S_2(TTF)S_2)Pt(PPh_3)_2]$ (TTF = tetrathiafulvalene).[44]

Reactions II and V by which compounds **3** are prepared essentially treat metal compounds **2** and **5** merely as protected "ligands," a point which suggests that new, higher nuclearity compounds could be prepared by simple addition of two or three ligand equivalents to a suitable metal halide. Thus, for instance, the introduction of 2 equiv of $[(dcpe)Ni(S_2C_6H_2S_2)]^{2-}$ to $NiCl_2$ or to $PtCl_2$, followed by addition of 1 equiv of I_2, leads to precipitation of the trimetallic compounds $[(dcpe)Ni(S_2C_6H_2S_2)]_2Ni$ (**6a**) or $[(dcpe)Ni(S_2C_6H_2S_2)]_2Pt$ (**6b**). Compounds **6a** and **6b** are appreciably darker in color than the mono- and dimetallic compounds, consistent with the formation of a greater extended delocalized electronic structure. Although sparing in their solubility in common organic solvents, **6a** and **6b** are sufficiently soluble in *N*,*N*-dimethylformamide (DMF) as to crystallize readily in the form of large prisms upon diffusion of ethereal solvent vapors. Apart from the $[[(edo)Ni(tto)]_2Ni]^{2-}$ and $[[(dddt)Ni(tto)]_2Ni]^{2-}$ dianions (edo(2-) = 5,6-dihydro-1,4-dioxine-2,3-dithiolate; dddt(2-) = 5,6-dihydro-1,4-dithine-2,3-dithiolate) recently isolated and characterized by Kato and co-workers,[13] compounds **6a** and **6b** are the only well-defined metal dithiolene compounds consisting of three metal atoms linked via bridging bis(dithiolene) ligands.

Elemental analysis data for compounds **2a**-**2d**, **3a**-**3d**, **6a**, and **6b** that are consistent with bulk sample purity have been difficult to obtain despite their characterization by spectroscopic means and by X-ray crystallography. We are inclined to the view, however, that the sample purities for these compounds may be better than suggested by the analytical data. One complication afflicting some of these compounds, **6a** for example, is their co-crystallization with multiple solvent molecules whose number and identity are unclear because of their highly disordered nature. Thus, these solvent molecules are impossible to account for analytically. Adding further to the challenge is the fact that compounds **2** and **6** are centrosymmetric and amply substituted with phenyl or cyclohexyl groups, which greatly diminishes their inherent solubility in common organic solvents. This poor solubility makes the complete redissolution, drying, and recovery of a crystalline sample of adequate mass very difficult to achieve. An additional problem that may be obscuring the actual purity of some of these new compounds is an interference by phosphorus with sulfur analyses, a complicating issue with sulfur analyses that has been noted in the analytical literature.[45] In the case of compound **2b**, for example, carbon and hydrogen analyze well, as expected for the spectroscopic purity that was indicated for the compound, but sulfur analyzes for a somewhat higher value than calculated. It is plausible that this discrepancy can be attributed to an interfering effect by phosphorus.

Structures. The structures of **2a**-**2d** have been determined (Table 1) and observed to have the square planar coordination geometries expected for a d^8 metal in the strong ligand field environment presented by dithiolene and chelating bis(phosphine) ligands. Previous structural studies of this molecule type have been limited to compounds with the 1,2-bis(diphenylphosphino)ethane[46−53] or 1,2-bis(diphenylphosphino)methane[54] ligands. Thermal ellipsoid plots of **2c** and **2d** are displayed in Figure 1; those of **2a**, **2b**, and **2e**, which are atom-labeled in a

(42) Abel, E. W.; Jenkins, C. R. *J. Chem. Soc. A* **1967**, 1344–1346.
(43) Usón, R.; Vicente, J.; Oro, J. *Inorg. Chim. Acta* **1981**, *52*, 29–34.
(44) McCullough, R. D.; Belot, J. A. *Chem. Mater.* **1994**, *6*, 1396–1403.
(45) Ma, T. S.; Rittner, R. C. *Modern Organic Elemental Analysis*; Marcel Dekker: New York, 1979; pp 211−212.
(46) Velázquez, C. S.; Baumann, T. F.; Olmstead, M. M.; Hope, H.; Barrett, A. G. M.; Hoffman, B. M. *J. Am. Chem. Soc.* **1993**, *115*, 9997–10003.
(47) Tian, Z.-Q.; Donahue, J. P.; Holm, R. H. *Inorg. Chem.* **1995**, *34*, 5567–5572.
(48) Kaiwar, S. P.; Hsu, J. K.; Liable-Sands, L. M.; Rheingold, A. L.; Pilato, R. S. *Inorg. Chem.* **1997**, *36*, 4234–4240.
(49) Chesney, A.; Bryce, M. R.; Batsanov, A. S.; Howard, J. A. K. *Chem. Commun.* **1997**, 2293–2294.
(50) Darkwa, J. *Inorg. Chim. Acta* **1997**, *257*, 137–141.
(51) Landis, K. G.; Hunter, A. D.; Wagner, T. R.; Curtin, L. S.; Filler, F. L.; Jansen-Varnum, S. A. *Inorg. Chim. Acta* **1998**, *282*, 155–162.
(52) Nihei, M.; Kurihara, M.; Mizutani, J.; Nishihara, H. *J. Am. Chem. Soc.* **2003**, *125*, 2964–2973.
(53) Ni, C.-L.; Li, Y.-Z.; Ni, Z.-P.; Dang, D.-B.; Meng, Q.-J. *Acta Crystallogr., Sect. E.* **2004**, *60*, m410–m412.
(54) Kang, B.-S.; Chen, Z.-N.; Gao, H.-R.; Zhou, Z.-Y.; Wu, B.-M.; Mak, T. M. C.; Lin, Z. *Huaxue Xuebao* **1998**, *56*, 58–67.

Table 1. Crystal and Refinement Data for Compounds **2a**−**d**, **3ab**, **3d**−**f**, $[\mathbf{3d}]^+$, $[\mathbf{4c}]^{2+}$, **5d**, **6ab**, **7d**

	2a	**2b**	**2c**	**2d**	**3a**
solvent	none	none	1/2DCE	none	none
formula	$C_{33}H_{26}NiOP_2S_4$	$C_{33}H_{24}NiOP_2S_4$	$C_{33}H_{28}ClNiOP_2S_4$	$C_{33}H_{50}NiOP_2S_4$	$C_{58}H_{50}Ni_2P_4S_4$
fw	687.43	685.41	784.94	711.62	1116.52
xtl system	orthorhombic	orthorhombic	monoclinic	monoclinic	monoclinic
space grp	$P2_12_12_1$	$P2_12_12_1$	$P2_1/c$	$P2_1/c$	$P2_1/n$
color, habit	orange plate	red block	orange plate	orange plate	orange-brown block
a, Å	11.155(3)	9.872(2)	9.048(2)	12.065(2)	11.320(3)
b, Å	12.849(3)	15.547(3)	21.139(5)	17.391(3)	15.354(4)
c, Å	21.133(5)	19.629(4)	18.511(4)	16.307(3)	14.681(4)
α, deg.	90	90	90	90	90
β, deg.	90	90	95.679(3)	102.639(3)	103.202(5)
γ, deg.	90	90	90	90	90
V, Å^3	3029(1)	3013(1)	3523(1)	3338.6(9)	2484(1)
T, K	100	100	100	100	100
Z	4	4	4	4	2
R1, wR2[a]	0.0686, 0.1616	0.0267, 0.0628	0.0333, 0.0749	0.0460, 0.1065	0.0454, 0.1040
GoF	1.107	1.027	1.029	1.036	1.059

	3b	**3d**	**3e**	**3f**	**[3d][BArF$_{24}$]**
solvent	none	~3(C_6H_{14})[b]	2.5DCE[c]	4C_6H_5Cl·2DCE[c]	C_6H_5Cl
formula	$C_{58}H_{46}Ni_2P_4S_4$	$C_{58}H_{98}Ni_2P_4S_4$	$C_{60.5}H_{103}Cl_{2.5}NiP_4PdS_4$	$C_{86}H_{126}Cl_8P_4Pd_2S_4$	$C_{96}H_{115}BClF_{24}Ni_2P_4S_4$
fw	1112.49	1164.90	1336.28	1908.39	2140.68
xtl system	monoclinic	monoclinic	triclinic	tetragonal	monoclinic
space grp	$P2_1/n$	Pc	$P\bar{1}$	$P4_2/n$	$C2/c$
color, habit	orange-brown needle	red plate	red parallelpipeds	orange column	orange plate
a, Å	10.971(2)	11.115(2)	12.054(1)	29.076(3)	32.915(9)
b, Å	15.318(3)	35.667(6)	25.100(2)	29.076(3)	14.480(4)
c, Å	15.200(3)	17.500(3)	25.131(2)	11.430(1)	51.18(1)
α, deg.	90	90	88.735(1)	90	90
β, deg.	100.976(4)	99.111(4)	82.764(1)	90	105.047(4)
γ, deg.	90	90	85.975(1)	90	90
V, Å^3	2507.5(8)	6851(2)	7524(1)	9664(2)	23550(10)
T, K	100	100	100	100	100
Z	2	4	4	4	8
R1, wR2[a]	0.0616, 0.1397	0.0810, 0.1589	0.0631, 0.1789	0.0587, 0.1391	0.0626, 0.1746
GoF	1.030	1.005	1.074	1.092	0.971

compound	**5d**	**6a**	**6b**	**7d**	**[4c][BArF$_{24}$]$_2$**
solvent	1/2DCE[c]	~3DME[b,d]	~3$CH_3C(OCH_3)_2CH_3$[b]	2−3CH_2Cl_2[b]	4$CHCl_3$
formula	$C_{41}H_{70}ClNiP_2S_4Sn$	$C_{64}H_{100}Ni_3P_4S_8$	$C_{64}H_{100}Ni_2P_4PtS_8$	$C_{64}H_{100}Ni_2P_4S_8$	$C_{200}H_{128}Ag_2B_2Cl_{12}F_{48}Ni_4P_8S_8$
fw	966.07	1425.93	1562.31	1367.22	4844.86
xtl system	monoclinic	rhombohedral	rhombohedral	monoclinic	triclinic
space grp	$P2_1/c$	$R\bar{3}$	$R\bar{3}$	$P2_1/n$	$P\bar{1}$
color, habit	orange column	brown-black block	brown-black block	yellow plate	orange plate
a, Å	38.367(3)	44.592(2)	45.13(1)	11.593(2)	11.682(4)
b, Å	10.3214(9)	44.592(2)	45.13(1)	15.536(3)	19.518(6)
c, Å	48.842(4)	41.023(3)	40.63(2)	21.865(4)	23.550(7)
α, deg.	90	90	90	90	86.004(4)
β, deg.	97.497(3)	90	90	94.771(2)	77.999(4)
γ, deg.	90	120	120	90	87.417
V, Å^3	19176(3)	70643(6)	71670(40)	3925(1)	5237(3)
T, K	100	100	100	100	100
Z	16	18	18	2	1
R1, wR2[a]	0.0806, 0.1687	0.0714, 0.1225	0.0755, 0.0998	0.0750, 0.1947	0.0754, 0.1930
GoF	1.086	1.029	1.026	1.004	1.039

[a] $R1 = \sum||F_o| - |F_c||/\sum|F_o|$. $wR2 = \{\sum w(F_o^2 - F_c^2)^2/\sum w(F_o^2)^2\}^{1/2}$; $w = 1/[\sigma^2(F_o^2) + (xP)^2]$, where $P = (F_o^2 + 2F_c^2)/3$. [b] Solvent was highly disordered and removed with the use of SQUEEZE in PLATON. [c] DCE = 1,2-dichloroethane. [d] DME = 1,2-dimethoxyethane.

fashion strictly analogous to **2c** and **2d**, are available in Supporting Information. Ni−S bond lengths range from 2.1481(6)−2.179(2) Å, while Ni−P bond lengths span a broader range from 2.1530(7)−2.1987(7) Å. The longest Ni−P bond lengths (2.1847(7), 2.1987(7) Å) occur in **2d** and are likely due to the greater closeness to idealized square planar geometry in this compound compared to **2a**-**2c**, as measured by the angle, θ, between the S(1)−Ni(1)−S(2) and P(1)−Ni(1)−P(2) planes (1.6°, Supporting Information, Table S1) and by the mean atom deviation, δ_m, from the S_2NiP_2 plane (0.012 Å, Supporting Information, Table S1). A consequence of the small tetrahedral distortion at Ni in **2d** is a greater *trans* influence exerted upon the phosphine ligand by the thiolate sulfur atoms of the dithiolene ligand.

Structural identification of arenetetrathiolate-linked dimetal compounds **3abdef** has also been accomplished (Table 1, Figure 1). The closest analogues to these compounds that have been crystallographically characterized are $[(\eta^5\text{-}C_5H_4(SiMe_3))M(S_2C_6H_2S_2)M(\eta^5\text{-}C_5H_4(SiMe_3))]$

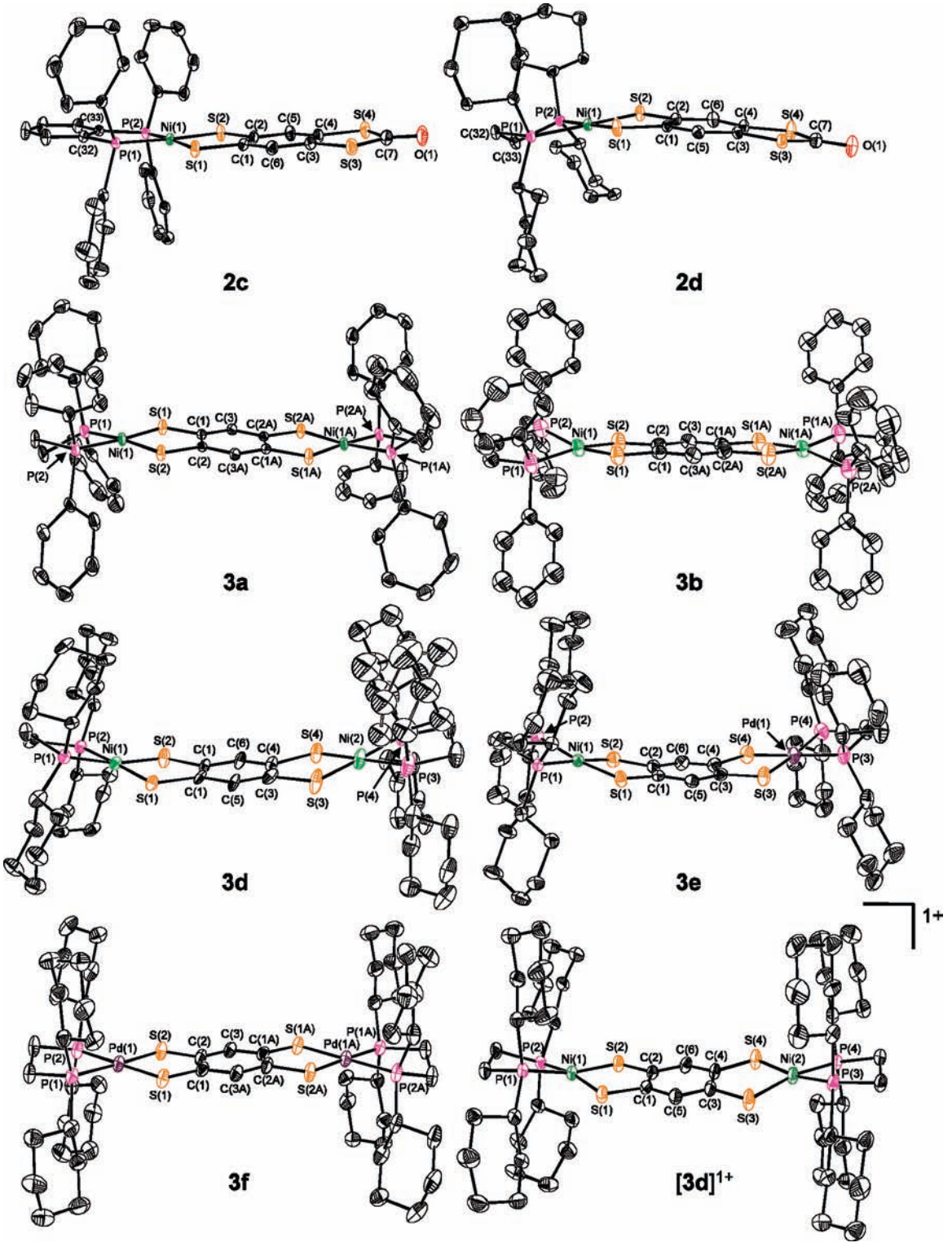

Figure 1. Structures of mononickel compounds **2c**, **2d** and dimetal compounds **3a**, **3b**, **3d**, **3e**, **3f**, and $[\mathbf{3d}]^{1+}$. Thermal ellipsoid plots are drawn at the 50% probability level. H atoms are omitted for clarity.

(M = Ti, Zr, Hf)[32b] and Cp*Co($S_2C_6H_2S_2$)CoCp*.[25] Compounds **3a** and **3b** crystallize on inversion centers in monoclinic space group $P2_1/n$ with similar unit cell dimensions. Compound **3b** differs from **3a** by revealing somewhat greater tetrahedralization at the nickel center, manifested by θ and δ_m values of 16.9° and 0.181 Å as compared to 4.9° and 0.053 Å for **3a** (Table 2). The structure of **3d** was solved in the non-centric space group *Pc* with two independent molecules in the asymmetric unit, each of which reveals a concave, end-to-end bending that precludes a symmetry center (Supporting Information, Figure S1). This saddle-shaped structure is apparently due to crystal packing effects, as opposed to stereoelectronic factors through which a distorted geometry ends up at lower energy than a more symmetric planar configuration. As seen in Supporting Information,

Table 2. Selected Averaged[a] Bond Distances (Å) and Angles (deg) for Compounds **3abdef** and $[\mathbf{3d}]^+$

	3a	3b	3d[b]	3e[b]	3f	$[\mathbf{3d}]^+$
M−S[c]	2.1686[6]	2.158[1]	2.172[1]	2.2358[5]	2.3105[7]	2.1695[5]
M−P[c]	2.1920[6]	2.154[1]	2.178[1]	2.2253[5]	2.2775[7]	2.1728[5]
S−C	1.758[1]	1.757[4]	1.789[4]	1.758[2]	1.765[3]	1.722[2]
chelate C−C	1.398(3)[d]	1.401(7)[d]	1.387[6]	1.403[4]	1.397(6)[d]	1.432[4]
intermetal dist., Å	8.518	8.447	8.489	8.505	8.759	8.412
S−M−S	91.58(3)[d]	92.76(6)[d]	91.38[5]	91.06[3]	88.88(4)[d]	92.02[3]
P−M−P	87.07(3)[d]	87.50(6)[d]	88.45[6]	87.73[3]	86.40(4)[d]	88.61[3]
P−M−S_{cis}	90.76[2]	91.10[4]	90.20[4]	90.70[2]	92.35[3]	90.37[2]
P−M−S_{trans}	175.79[2]	167.64[5]	175.51[5]	175.36[2]	178.55[3]	170.92[2]
δ_m, Å, S_2MP_2[e,f]	0.053	0.181	0.114	0.087	0.006	0.145
δ_m, Å, $S_2M'P_2$[f,g]			0.025	0.042		0.126
θ, deg.[h]	4.9	16.9	11.3	7.9	1.1	13.3
θ', deg.[i]			2.4	5.2		11.8
τ, deg.[j]	0	0	26.1	28.7	0	13.5
φ, deg.[k]	4.0	4.3	18.9	3.9	5.6	9.3

[a] Uncertainties for averaged values are computed according to the general formula for error propagation in a function of multiple variables as described by Taylor, J. R. *An Introduction to Error Analysis*; University Science Books: Sausalito, CA, 1997; pp 73−77. [b] Data are for one of two independent molecules in the asymmetric unit. [c] M = Ni for **3a**, **3b**, **3d**, $[\mathbf{3d}]^+$; M = Pd for **3f**; for **3e**, M = both Ni and Pd, which are disordered over the metal positions in a ~4:6 ratio. [d] Non-averaged values. [e] M = Ni(1) for **3a**, **3b**, **3d**, $[\mathbf{3d}]^+$; M = Pd(1) for **3f**; for **3e**, M = the metal atom position predominantly occupied by Ni(1), as illustrated in Figure 1. [f] Mean atom deviation from S_2MP_2 or $S_2M'P_2$ plane. [g] M′ = Ni(2) for **3d**, $[\mathbf{3d}]^+$; for **3e**, M′ = the metal atom position predominantly occupied by Pd(1), as illustrated in Figure 1. [h] Angle between the S(1)−M−S(2) and P(1)−M−P(2) planes. [i] Angle between the S(3)−M′−S(4) and P(3)−M′−P(4) planes. [j] Angle between mean S_2MP_2 planes. [k] End-to-end molecular twist, defined as absolute value of the P(1)−M(1)−M-(1A)−P(2A) or P(1)−M(1)−M′−P(3) torsion angle.

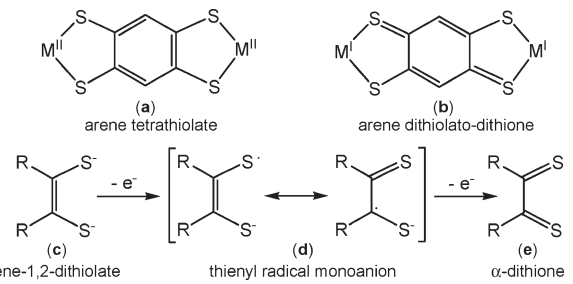

Figure 2. Possible formulations of metal and ligand oxidation states in compounds **3** (**a** and **b**); possible oxidation states of dithiolene ligands (**c**−**e**).

Figure S1, the (dcpe)Ni end groups of **3d** bend upward to accommodate the steric crowding of another molecule abutting its underside. Both Ni centers reveal some degree of tetrahedralization, although that for Ni(1) in **3d** is appreciably greater (Table 2) than that at Ni(2). Compounds **3a**, **3b**, and **3d** reveal S−C bond lengths ($S-C_{ave}$ = 1.757[4]−1.789[4] Å) that are consistent with bona fide single bonds and confirm the description of the bridging ligand as a fully reduced arene tetrathiolate, rather than as a dithiolato-dithione species with corresponding Ni(I) centers (Figure 2).

The structure of the mixed-metal compound **3e** is highly similar to that of **3d** and, as would be expected a priori, reveals a disorder of the Ni and Pd atoms over both metal sites. When the description of the molecule is not restricted to 1:1 distribution of each metal atom over the two sites, the refinement optimizes at a 40:60 distribution. In Figure 1, the Ni and Pd atoms are drawn in their predominant positions. The position with majority occupancy by Pd reveals somewhat *less* tetrahedralization than the site that is predominantly Ni. A DFT computational analysis of **3d** and **3e** (vide infra) predicts greater planarity at the Pd center, and this slight difference between the two ends of the molecule is possibly the basis by which the molecules find a way to pack themselves with a slight ordering rather than with complete randomization of the two ends. Crystallization of dipalladium compound **3f** occurred on an inversion center in tetragonal space group $P4_2/n$. This compound reveals almost perfect planarity from end-to-end with virtually no tetrahedralization at the metal atoms (Table 2), a contrast to the dinickel compounds.

Observations noted in the electrochemistry studies of compounds **3a-d**, for example, a pronounced sensitivity toward supporting electrolytes with small, potentially coordinating anions, suggested that the redox processes seen in these compounds are oxidations primarily localized on the arenetetrathiolate ligand that bridges the metal centers. The usefulness of crystallography in identifying ligand-based, as opposed to metal-based, redox events[55−60] thus made the isolation and structural study of a cationic form of one of these dimetallic compounds a particularly desirable objective. Use of $Ag[BArF_{24}]$ in CH_2Cl_2 as one-electron chemical oxidant of compounds **3** resulted in an immediate and noticeable change in color, implying that oxidation occurred. However, the formation of a diamagnetic species was suggested by ^{31}P NMR spectroscopy, an observation inconsistent with the unpaired spin of the intended product. When compound **3c** was subjected to this oxidation by $Ag[BArF_{24}]$, orange plate crystals serendipitously formed in the NMR tube that were of a quality suitable for X-ray diffraction. Crystallographic identification of this compound revealed it to be an unanticipated tetra-nickel species in which two molecules of **3c** are brought together in an

(55) Muresan, N.; Chlopek, K.; Weyhermüller, T.; Neese, F.; Wieghardt, K. *Inorg. Chem.* **2007**, *46*, 5327–5337.
(56) Patra, A. K.; Bill, E.; Weyhermüller, T.; Stobie, K.; Bell, Z.; Ward, M. D.; McCleverty, J. A.; Wieghardt, K. *Inorg. Chem.* **2006**, *45*, 6541–6548.
(57) Ray, K.; Bill, E.; Weyhermüller, T.; Wieghardt, K. *J. Am. Chem. Soc.* **2005**, *127*, 5641–5654.
(58) Ray, K.; Weyhermüller, T.; Goossens, A.; Crajé, M. W. J.; Wieghardt, K. *Inorg. Chem.* **2003**, *42*, 4082–4087.
(59) Herebian, D.; Bothe, E.; Neese, F.; Weyhermüller, T.; Wieghardt, K. *J. Am. Chem. Soc.* **2003**, *125*, 9116–9128.
(60) Sun, X.; Chun, H.; Hildenbrand, K.; Bothe, E.; Weyhermüller, T.; Neese, F.; Wieghardt, K. *Inorg. Chem.* **2002**, *41*, 4295–4303.

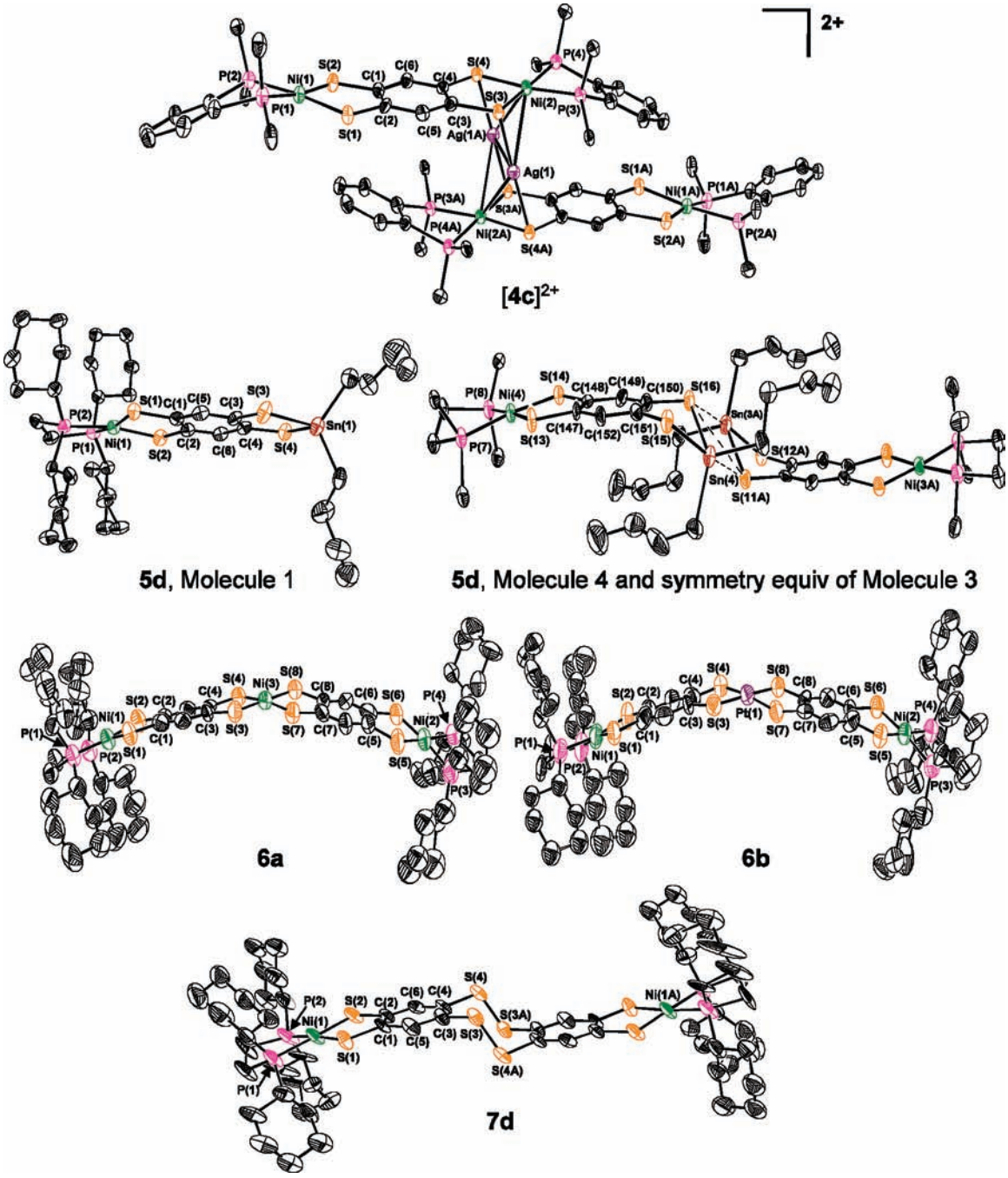

Figure 3. Thermal ellipsoid plot of dication $[\mathbf{4c}]^{2+}$, di-*n*-butyltin-protected compound **5d**, trinuclear compounds **6a** and **6b**, and bis(disulfide) linked compound **7d**. Ellipsoid plots are drawn at the 50% level for $[\mathbf{4c}]^{2+}$, **5d**, and **7d** and at the 40% level for **6a** and **6b**. H atoms are omitted for clarity. For $[\mathbf{4c}]^{2+}$ and **5d** (right side), phenyl and cyclohexyl groups on the phosphorus atoms are truncated for clarity.

offset face-to-face way and bridged via a Ag_2 unit that interacts with four arenethiolate sulfur atoms, two from each of the contributing **3c** halves (Figure 3, $[\mathbf{4c}]^{2+}$). This hexametallic species is a dication with two corresponding $[BArF_{24}]^-$ counteranions. An inversion center occurs at the midpoint of the 2.996(1) Å Ag···Ag interatomic separation such that only one silver atom and one of the **3c** "halves" is crystallographically unique. The average S−C and chelate C−C bond lengths in $[\mathbf{4c}]^{2+}$ (1.764[4] and 1.405[7] Å, respectively, Table 3) are not significantly different than those found in molecules **3abd** (Table 2) and indicate that electron transfer did not occur from the arenetetrathiolate unit as intended. Instead, the two Ag^+ cations are stabilized in close proximity by thiophilic interactions with the electron-rich reduced sulfur atoms. The redox potential of the Ag^+/Ag couple is well-known to be a function of solvent donor ability.[61] In the presence of soft donor groups such as those afforded by the arenetetrathiolate ligand, it apparently is diminished to a value that is smaller than the $[\mathbf{3c}]^+/\mathbf{3c}$ couple. Structures analogous to $[\mathbf{4c}]^{2+}$ have been observed with similar $Ag^+\cdots Ag^+$ distances, selected examples being

(61) Connelly, N. G.; Geiger, W. E. *Chem. Rev.* **1996**, *96*, 877–910.

Table 3. Selected Averaged[a] Interatomic Distances and Angles for $[\mathbf{4c}]^{2+}$

Ni(1)−S	2.155[1]	S−Ni(1)−P_{cis}	91.05[6]
Ni(1)−P	2.155[2]	S−Ni(1)−P_{trans}	172.40[7]
Ni(2)−S	2.170[1]	S(3)−Ni(2)−S(4)[b]	92.80(8)
Ni(2)−P	2.175[1]	P(3)−Ni(2)−P(4)[b]	83.86(8)
Ni(2)−Ag	2.9490[7]	S−Ni(2)−P_{cis}	91.54[6]
S−Ag	2.441[1]	S−Ni(2)−P_{trans}	174.03[6]
Ag(1)−Ag(1A)[b]	2.996(1)	Ag(1)−Ni(2)−Ag(1A)[b]	61.05(3)
S−C	1.764[4]	S(3)−Ni(2)−Ag(1)[b]	54.03(6)
chelate C−C	1.405[7]	S(4)−Ni(2)−Ag(1A)[b]	54.80(6)
Ni(1)···Ni(2)	8.439	S(3)−Ni(2)−Ag(1A)[b]	98.69(7)
Ni(2)···Ni(2A)	5.080	S(4)−Ni(2)−Ag(1)[b]	99.00(7)
δ_m, Ni(1), Å[c]	0.101	θ, Ni(1), deg.[d]	9.5
δ_m, Ni(2), Å[c]	0.024	θ, Ni(2), deg.[d]	5.5
		τ, Ni(1), deg.[e]	
S(1)−Ni(1)−S(2)[b]	93.09(9)	τ, Ni(2), deg.[e]	7.9
P(1)−Ni(1)−P(2)[b]	85.44(9)	φ, deg.[f]	0

[a] Uncertainties for averaged values are computed according to the general formula for error propagation in a function of multiple variables as described by Taylor, J. R. *An Introduction to Error Analysis*; University Science Books: Sausalito, CA, 1997; pp 73−77. [b] Non-averaged value. [c] Mean atom deviation from S_2NiP_2 plane. [d] Angle between S_2Ni and P_2Ni planes. [e] Angle between mean S_2NiP_2 plane and mean $S_2C_6S_2$ plane. [f] Angle between mean $S_2C_6S_2$ planes.

$[[(Ph_3P)_2Pt(S_2C_{10}H_6)]_2(\mu\text{-}Ag_2)]^{2+}$,[62] and $[[Cp^*Ru(tpdt)]_2(\mu\text{-}Ag_2)]^{2+}$ (tpdt = 3-thiapentane-1,5-dithiolate).[63]

Structural identification of $[\mathbf{4c}][BArF_{24}]_2$ clarified the need for an innocent, outer-sphere electron transfer reagent for the preparation of $[\mathbf{3d}]^+$. Reaction of **3d** with $[Cp_2Fe][BArF_{24}]$ as oxidizing agent resulted in immediate darkening of color and formation of a product with greater solubility than the charge-neutral starting compound. Crystals grown by the vapor diffusion technique were examined by X-ray diffraction and found to be the desired monocationic species, $[\mathbf{3d}]^+$, without any perturbing influences being exerted upon the tetrathiobenzene unit. The averaged S−C and chelate C−C bond distances for $[\mathbf{3d}]^+$ (1.722[2] and 1.432[4] Å, Table 2) are seen to be shorter and longer, respectively, than the corresponding values for **3d** (1.789[4] and 1.387[6] Å, Table 2) by a degree that is significant within the resolution of the experimental data. Thus, the removal of an electron from a fully reduced ene-1,2-dithiolate has occurred, with the result that the S−C bonds now have partial thione character while the C−C chelate bond lengths have some admixture of single bond quality (**d** in Figure 2).

As noted earlier, compound **5d** was examined as an alternative synthon to compound **2d**. Although a variety of dithiolene ligands masked with dialkyl tin protecting groups have been crystallographically identified,[64−66] **5d** represents the first structural characterization of a bis(dithiolene) type molecule in which one dithiolene chelate is coordinated to a transition metal while the other remains protected with a dialkyl tin group and is available for further chemistry. A molecule analogous to **5d**, $Cp^*Co(S_2C_6H_2S_2)Sn^nBu_2$, has been recently described by Nomura and Fourmigué and constitutes the only other such example.[25] The asymmetric unit for **5d** is composed of four independent molecules, two of which are completely noninteracting with anything and hold the tetrahedral Sn atoms approximately in the same plane as the $S_2C_6H_2S_2$ bridging ligand. The remaining two molecules of **5d** show a pronounced folding of the Sn^nBu_2 fragment upward along the S···S interatomic axis of the two sulfur atoms coordinated to tin. This different conformation is due to a weak intermolecular interaction with the thiolate sulfur of another molecule such that the tin atoms are pseudo-pentacoordinate (Figure 3). These two conformations have been independently observed in different crystal structures of $R_2C_2S_2SnR'_2$ compounds[64−66] but not simultaneously within the same crystal structure. Selected bond lengths and angles for **5d** are presented in Supporting Information, Table S4.

Table 4. Selected Averaged[a] Bond Distances (Å) and Angles (deg) for Trimetallic Compounds **6a** and **6b**

	6a	6b		6a	6b
$Ni_{term}-S$[b]	2.161[1]	2.151[2]	S−Ni−S_{term}[b]	92.29[6]	92.67[9]
M−S[c]	2.141[1]	2.228[2]	P−Ni−P	89.03[6]	88.3[1]
Ni−P	2.168[1]	2.159[2]	S−Ni−P_{cis}	89.70[4]	89.97[8]
S−C_{term}[b]	1.741[4]	1.716[6]	S−Ni−P_{trans}	173.13[5]	172.51[9]
S−C_{cent}[d]	1.730[4]	1.726[5]	chelate S−M−S[c]	92.66[6]	89.80[8]
chelate C−C_{term}[b]	1.393[6]	1.369[9]	S−M−S_{cis}[c]	87.37[6]	90.06[8]
chelate C−C_{cent}[d]	1.395[6]	1.392[8]	S−M−S_{trans}[c]	174.34[6]	174.61[9]
Ni(1)···Ni(2), Å	16.5	16.6	θ, Ni(1), deg.[e]	8.3	12.3
δ_m, Ni(1), Å[f]	0.090	0.133	θ, Ni(2), deg.[e]	10.2	7.5
δ_m, Ni(2), Å[f]	0.111	0.081	θ, M, deg.[e,f]	9.4	7.6
δ_m, M, Å[e,e]	0.086	0.052	β, deg.[g]	46.5	46.7
			τ, deg.[h]	20.9	23.5

[a] Uncertainties for averaged values are computed according to the general formula for error propagation in a function of multiple variables as described by Taylor, J. R. *An Introduction to Error Analysis*; University Science Books: Sausalito, CA, 1997, pp 73−77. [b] Bond length or angle for terminal nickel or nickel dithiolene chelate. [c] M = Ni(3) for **6a**, Pt(1) for **6b**; [d] Bond length or angle for central metal or metal dithiolene chelate. [e] Angle between S_2Ni and P_2Ni or S_2M and S_2M planes. [f] Mean atom deviation from S_2NiP_2 or S_4M plane. [g] Angle between $S_2Ni(1)P_2$ and $S_2Ni(2)P_2$ mean planes. [h] End-to-end molecular twist, defined as the P(1)−Ni(1)−Ni(2)−P(3) torsion angle.

Trimetallic compounds **6a** and **6b**, owing to solubility limitations, could only be crystallized from DMF solutions. The diffusion of various types of ethers into DMF solutions readily formed large, dark, prism-shaped crystals that displayed only weak diffraction because of a high degree of solvent disorder. Both **6a** and **6b** solved in rhombohedral space group $R\bar{3}$ and are essentially isomorphous. To our knowledge, **6a** and **6b** comprise only the second set of well characterized trimetallic molecules in which metal atoms are linked with bis(dithiolene) ligands. A pair of trimetallic anions with metal atoms linked by tetrathiooxalate anions and capped with dithiolene end groups was recently described by Kato et al.[13] Both molecules **6a** and **6b** display an appreciable end-to-end bending of ~46° (Table 4) in addition to a twisting or corkscrewing of ~20° along the 22 Å length of the molecule (Table 4). These deformations, somewhat surprising in their magnitude, completely obviate any molecular center of symmetry.

Bis(disulfide)-linked compounds **7c** and **7d**, were identified in the course of exploring the Rxn III synthesis for compounds **3**. These compounds both crystallize upon inversion centers and display parallel planar arene

(62) Robertson, S. D.; Slawin, A. M. Z.; Woollins, J. D. *Eur. J. Inorg. Chem.* **2007**, 247–253.
(63) Shin, R. Y. C.; Tan, G. K.; Koh, L. L.; Vittal, J. J.; Goh, L. Y.; Webster, R. D. *Organometallics* **2005**, *24*, 539–551.
(64) Allan, G. M.; Howie, R. A.; Skakle, J. M. S.; Wardell, J. L.; Wardell, S. M. S. V. *J. Organomet. Chem.* **2001**, *627*, 189–200.
(65) Ma, C.; Han, Y.; Li, D. *Polyhedron* **2004**, *23*, 1207–1216.
(66) Chandrasekaran, P.; Arumugam, K.; Jayarathne, U.; Pérez, L. M.; Mague, J. T.; Donahue, J. P. *Inorg. Chem.* **2009**, *48*, 2103–2113.

tetrathiolate groups that are separated by 2.06 Å, the length of the disulfide bonds. This configuration imposes a chairlike conformation upon the central $S_2C_2S_2C_2$ ring (Figure 3). Various examples of purely organic bis-(disulfide)-linked bis(arenes) have been reported,[67−72] but compounds **7** appear to be the only instances of metal-containing molecules of this type. The intermetal distance in **7d** is 14.6 Å, while the total end-to-end length of the molecule is ~21 Å. In principle, compounds **7** could serve as yet another form of protected nickel dithiolene complex, analogous to compounds **2** and to **5d**, but with four reducing equivalents being required to liberate the two halves as fully reduced ene-1,2-dithiolates. Selected structural parameters for compound **7c** and **7d** are available in the Supporting Information, Table S6.

Electrochemistry. Mononickel mixed dithiolene and bis(phosphine) complexes have been studied in some detail and generally found to sustain a reversible Ni(II) → Ni(I) reduction and, in the particular case of the phenyl-substituted dithiolene ligand, a reversible oxidation assigned as an ene-1,2-dithiolate to thioketyl ligand-based oxidation.[40] The less electron-rich $S_2C_2(CN)_2$ and tdt (tdt = toluene-3,4-dithiolate) ligands were not observed to support reversible oxidation in [(P-P)Ni-$(S_2C_2R_2)$] complexes.[39] The known electron richness of the tetrathioarene unit,[73,74] manifested by the oxidation waves at +1.17 V and +1.68 V that it reveals protected as the tetra(isopropylthio)benzene (Figure 4), suggests at the outset the possibility for reversible anodic electrochemistry. Cyclic voltammetry upon mononickel compound **2d** with $[Bu_4N][PF_6]$ electrolyte reveals a single reversible oxidation wave at 0.82 V, a potential 0.35 V less oxidizing than the first feature observed for 1,2,4,5-$(^i$PrS$)_4C_6H_2$ (Figure 4). If this oxidation in **2d** is indeed occurring at the tetrathioarene moiety, this shift in potential indicates that the electron-withdrawing nature of the carbonyl protecting group at the other end of the arene ring is more than offset by an electron-donating character of the (dcpe)Ni fragment. Differential pulse voltammograms for **2a**−**2d** are presented in Figure 5. Somewhat surprisingly in light of the reversibility seen for **2d**, compounds **2a**−**2c** display no reversible behavior in their cyclic voltammograms.

The dinickel compounds **3a**−**3d** reveal increased redox activity at milder potentials than for the corresponding compounds **2a**−**d**. Compound **3d**, for example, shows two fully reversible oxidations at 0.18 and 0.84 V (vs Ag/AgCl) in CH_2Cl_2 with $[Bu_4N][PF_6]$ as supporting

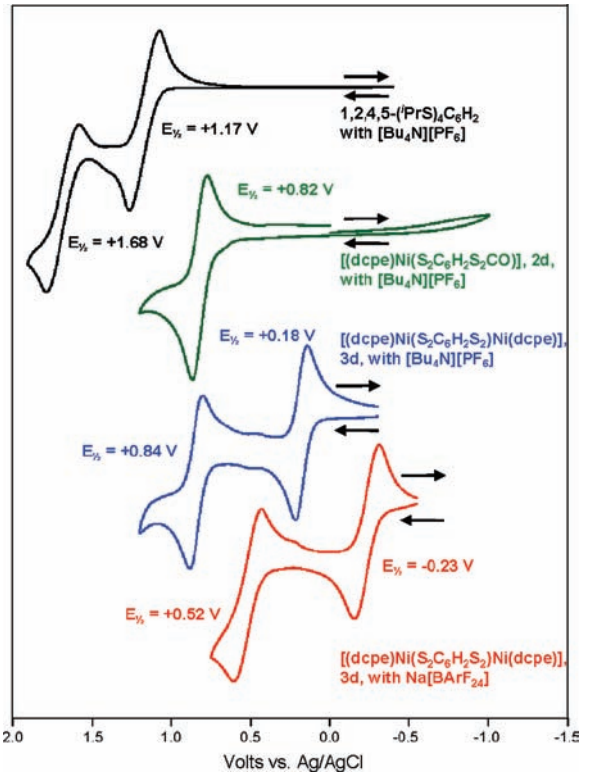

Figure 4. Cyclic voltammetry for 1,2,4,5-$(^i$PrS$)_4C_6H_2$, [(dcpe)Ni-$(S_2C_6H_2S_2CO)$] and [(dcpe)Ni$(S_2C_6H_2S_2)$Ni(dcpe)]. The solvent was CH_2Cl_2 for scans with $[Bu_4N][PF_6]$ electrolyte and 5:4:1 CH_2Cl_2/anisole/THF for scans with Na$[BArF_{24}]$.

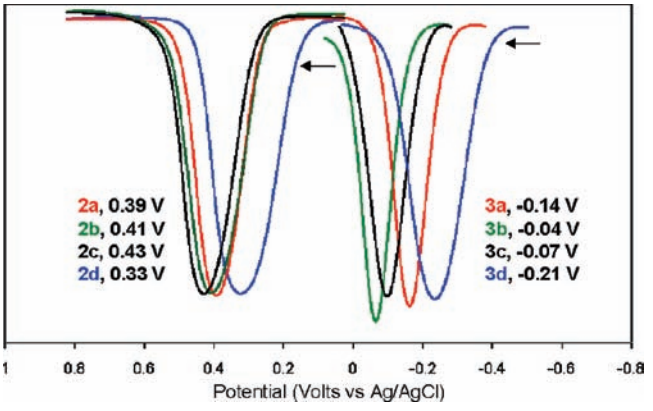

Figure 5. Overlay differential pulse voltammograms for compounds **2a**−**2d** and for the first oxidation wave for compounds **3a**−**3d**. For compounds **2**, scans were run in CH_2Cl_2 with 0.01 M Na$[BArF_{24}]$; only the oxidation for **2d** is reversible. For compounds **3**, scans were run in 5:4:1 CH_2Cl_2/anisole/THF with Na$[BArF_{24}]$.

electrolyte (Figure 4, Table 5). The $\Delta E_{1/2}$ value of 0.66 V corresponds to a comproportionation constant, K_c, of 1.6×10^{11} for the $[\mathbf{3d}]^{2+} + \mathbf{3d} \leftrightarrow 2[\mathbf{3d}]^{+}$ equilibrium.[75] Comproportionation constants of this magnitude are attributed to a high degree of charge delocalization within the mixed valence species. An assignment of the arene tetrathiolate ligand as the redox active moiety is consistent with this K_c value because the hole created by ligand oxidation is distributed among the four sulfur atoms, which are chemically indistinguishable.

(67) Lakshmikantham, M. V.; Raasch, M. S.; Cava, M. P.; Bott, S. G.; Atwood, J. L. *J. Org. Chem.* **1987**, *52*, 1874–1877.
(68) Chivers, T.; Parvez, M.; Vargas-Baca, I.; Schatte, G. *Can. J. Chem.* **1998**, *76*, 1093–1101.
(69) Ogawa, S.; Sugawara, M.; Kawai, Y.; Niizuma, S.; Kimura, T.; Sato, R. *Tetrahedron Lett.* **1999**, *40*, 9101–9106.
(70) Kimura, T.; Mizusawa, S.; Yoneshima, A.; Ito, S.; Tsujimura, K.; Yamashita, T.; Kawai, Y.; Ogawa, S.; Sato, R. *Bull. Chem. Soc. Jpn.* **2002**, *75*, 2647–2653.
(71) Yamamoto, T.; Ogawa, S.; Sugawara, M.; Kawai, Y.; Sato, R. *Bull. Chem. Soc. Jpn.* **2006**, *79*, 460–467.
(72) Yearley, E. J.; Lippert, E. L.; Mitchell, D. J.; Pinkerton, A. A. *Acta Crystallogr., Section C.* **2007**, *63*, o576–o577.
(73) Alberti, A.; Pedulli, G. F.; Tiecco, M.; Testaferri, L.; Tingoli, M. *J. Chem. Soc., Perkin Trans. II* **1984**, 975–979.
(74) Nabeshima, T.; Iwata, S.; Furukawa, N.; Morihashi, K.; Kikuchi, O. *Chem. Lett.* **1988**, 1325–1328.
(75) Richardson, D. E.; Taube, H. *Inorg. Chem.* **1981**, *20*, 1278–1285.

Table 5. Electrochemical Data for Compounds **2a**−**d** and **3a**−**d**

	2a	**2b**	**2c**	**2d**
0 → 1+ [a]				0.82 V
0 → 1+ [b]	0.39 V[c]	0.41 V[c]	0.43 V[c]	0.33 V
	3a	**3b**	**3c**	**3d**
0 → 1+ [a]				+0.18 V
0 → 1+ [d]	−0.14 V	−0.04 V	−0.11 V	−0.23 V
0 → 1+ [e]	−0.14 V	−0.04 V	−0.07 V	−0.21 V
1+ → 2+ [a]				+0.84 V
1+ → 2+ [d]				+0.52 V
1+ → 2+ [e]	0.55 V[c]	[f]	0.68 V[c]	+0.51 V

[a] Data obtained by CV in CH_2Cl_2 with 0.10 M Bu_4NPF_6 electrolyte. [b] Data obtained by DPV in CH_2Cl_2 with 0.01M $Na[BArF_{24}]$. [c] Irreversible. [d] Data obtained by CV in 5:4:1 CH_2Cl_2:anisole:THF with 0.01 M $Na[BArF_{24}]$ electrolyte. [e] Data obtained by DPV in 5:4:1 CH_2Cl_2:anisole:THF with 0.10 M Bu_4NPF_6 electrolyte. The Fc^+/Fc couple occurred at +0.54 V (by CV) in CH_2Cl_2 with 0.10 M Bu_4NPF_6 supporting electrolyte, at +0.20 V (by DPV) in CH_2Cl_2 with 0.01 M $Na[BArF_{24}]$, and at +0.30 V (by CV) in 5:4:1 CH_2Cl_2:anisole:THF with 0.01 M $Na[BArF_{24}]$ supporting electrolyte. [f] A consistent, reliable value for a second oxidation could not be obtained under the same conditions as used for **3a**, **3c**, and **3d**.

Repeated scanning over a period of minutes leads to appreciable degradation in the voltammogram of **3d** and eventually complete loss of observable current. This deterioration in the voltammogram is not accompanied by any change in the color or aspect of the analyte solution. The foregoing observations are indicative of sample degradation at the working electrode surface and consequent passivation of the electrode. Consistent with these observations, a quick removal and cleaning of the electrode surface restores the voltammetry to its initial, reversible-looking character.

Reactivity between solution-generated radical cations and small electrolyte anions that can act as nucleophiles, such as PF_6^-, BF_4^-, and ClO_4^-, has been noted by others and circumvented by use of large, weakly coordinating anions, such as $Na[BArF_{24}]$, as electrolyte medium.[76−80] When this particular salt is used as supporting electrolye in the voltammetry of **3d**, the oxidation waves are shifted some 0.30 V in the cathodic direction (Figure 4) and rendered well-behaved and stable toward an indefinite number of scans. A lack of solubility of compounds **3a**−**d** and the $Na[BArF_{24}]$ electrolyte in a common solvent has necessitated the use of a mixed solvent system. While $Na[BArF_{24}]$ is poorly soluble in CH_2Cl_2, it displays good solubility in ethereal solvents such as anisole; the inverse is true for compounds **3a**−**d**. The use of modest amounts of THF (≤10%) was observed empirically to improve the reversibility of the first oxidation wave in compounds **3a**−**d**, probably because of a stabilizing donor effect exerted by the THF solvent upon the radical monocation that is generated by the first oxidation. Thus, an optimal solvent system for compounds **3a**−**d** with $Na[BArF_{24}]$ is 5:4:1 CH_2Cl_2/anisole/THF, conditions under which the Fc^+/Fc couple occurs at 0.30 V. Only **3d** shows a second oxidation that appears reversible and is stable to repeated scanning. Figure 5 shows overlaid DPV for the first oxidations in compounds **3a**−**d** and reveals a similar range in oxidation potentials as seen for the series of mononickel compounds **2a**−**d**. The mildest oxidation potential is found for **3d**, the compound with the most electron-rich chelating diphosphine, while slightly stronger oxidizing potentials are required to transform compounds **3a**−**3c** to their corresponding cations. Considering the appreciable difference in basicity between dcpe and dppb, the relatively narrow range of 0.14 V in potentials suggests that metal-based Ni^{2+}/Ni^{3+} oxidations do not occur. Were the Ni^{2+} centers the site of oxidation, they might be expected to reveal greater sensitivity to the identity of the phosphine ligand.[37]

Calculations and Absorption Spectra. To better understand the deformations from idealized D_{2h} point group symmetry in compounds **3** and **6**, as well as to better see the composition of the redox active and spectroscopically active MOs, DFT calculations were undertaken using simplified models for compounds **3** and **6** in which monodentate phosphines, PH_3 or PMe_3, replace the chelating bis(phosphine) ligands. These calculations indicate that the idealized D_{2h} geometry for compounds **3** is a second order saddle point on the energy surface of the molecule. The molecule has an A_u symmetric vibration of imaginary frequency, which carries it to a lower symmetry D_2 geometry, in which point group the highest occupied molecular orbital (HOMO, (b_{2g}) and lowest unoccupied molecular orbital (LUMO) (b_{2u}) both reduce to the b_2 symmetry species; as a consequence, configuration interaction occurs, and the HOMO is lowered in energy. An imaginary frequency vibration of B_{3g} symmetry similarly carries the molecule to the C_{2h} point group, a symmetry in which both the HOMO and LUMO+1 belong to the b_g irreducible representation and thus undergo a completely analogous configuration interaction (Figure 6, (a)). Both the D_2 and C_{2h} geometries are energy minima and are lower in energy by 2.0 and 2.8 kcal/mol, respectively, than the D_{2h} geometry. These symmetry lowerings to D_2 and C_{2h}, which are instances of the second-order Jahn−Teller effect,[81] are produced by localized tetrahedralizing distortions at the nickel centers and are to be distinguished from the end-to-end folding observed in the structure of **3d**, a distortion *not* reproduced by the calculations and attributed instead to crystal packing (vide supra). Images (**b**) in Figure 6 clarify the distinction between the D_2 and C_{2h} geometries; the end-on view of the model compound along the Ni−Ni axis shows the P−Ni−P planes to be canted in opposite directions with respect to the $S_2C_6H_2S_2$ plane in D_2, while in C_{2h}, the P−Ni−P planes are canted in the same direction, one eclipsing the other.

Geometry optimization of the nickel−palladium bimetallic $[(H_3P)_2Ni(S_2C_6H_2S_2)Pd(PH_3)_2]$ compound (Figure 7, **3e′**) converged to an energy minimum with a nonplanar structure that closely approaches C_2 symmetry. The coordination geometry about palladium is nearly perfectly planar, as is common for Pd^{II}. The geometry at

(76) Zoski, C. G.; Sweigart, D. A.; Stone, N. J.; Rieger, P. H.; Mocellin, E.; Mann, T. F.; Mann, D. R.; Gosser, D. K.; Doeff, M. M.; Bond, A. M. *J. Am. Chem. Soc.* **1988**, *110*, 2109–2116.
(77) Hill, M. G.; Lamanna, W. M.; Mann, K. R. *Inorg. Chem.* **1991**, *30*, 4687–4690.
(78) LeSuer, R. J.; Geiger, W. E. *Angew. Chem., Int. Ed.* **2000**, *39*, 248–250.
(79) Camire, N.; Nafady, A.; Geiger, W. E. *J. Am. Chem. Soc.* **2002**, *124*, 7260–7261.
(80) Barrière, F.; Geiger, W. E. *J. Am. Chem. Soc.* **2006**, *128*, 3980–3989.
(81) Bersuker, I. B. *Chem. Rev.* **2001**, *101*, 1067–1114.

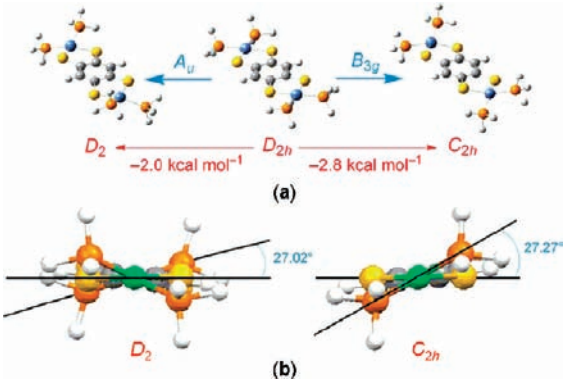

Figure 6. (**a**) Illustration of model compound $[(PH_3)_2Ni(S_2C_6H_2S_2)Ni(PH_3)_2]$ used in DFT calculations for compounds **3** and the molecular vibrations that result in lower symmetry through configuration interaction. (**b**) End-on views of the D_2 and C_{2h} symmetric compounds for emphasis of their difference.

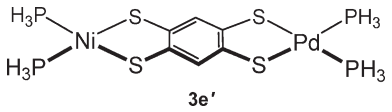

3e′

Figure 7. Model compound used for calculations on mixed metal compound **3e**.

nickel is distorted as in the dinickel complexes. The Ni coordination geometry is again intermediate between square planar and tetrahedral. The P−P−S−S dihedral angle at nickel is 26.8°; the opposite angle at palladium is 1.1°. Geometry optimization in full C_{2v} symmetry (that is, with all non-H atoms rigidly coplanar) converges to a first-order saddle point with an A_2 vibration of imaginary frequency. This normal mode is effectively localized at nickel, and carries the metal center out of a planar configuration toward a tetrahedral structure.

In planar (C_{2v}) **3e′**, the HOMO has b_1 symmetry and the LUMO is b_2. The imaginary-frequency A_2 vibration degrades the overall symmetry to C_2, wherein both orbitals transform as b. In planar **3e′**, the HOMO−LUMO separation is 0.896 eV, a small energy gap that favors orbital mixing by configuration interaction. Planar **3e′** also undergoes a second-order Jahn−Teller distortion that drives it toward a nonplanar geometry. The two metal atoms contribute equally to the electron density of the HOMO in the planar structure: 4.5% and 4.6% for Ni and Pd, respectively. The LUMO has greater nickel character: 28.3% Ni compared to 7.4% Pd. Upon distorting to C_2 symmetry, the HOMO gains Ni character at the expense of the LUMO. The HOMO has 8.7% Ni and 3.8% Pd electron density; the LUMO, 19.1 and 13.9%, respectively. Distortion from (planar) C_{2v} to (nonplanar) C_2 symmetry stabilizes **3e′** by 1.8 kcal mol^{-1}.

That the planar → nonplanar distortion localizes at nickel manifests the weaker ligand-field of the first-row metal and the predominance of a low-spin (square-planar and diamagnetic) ground state for palladium(II).[82] The phosphorus ligands in model complex **3e′** are PH_3, and the parent phosphine is one of the least nucleophilic phosphine ligands.[83] To investigate the structural

(82) Figgis, B. N.; Hitchman, M. A. *Ligand Field Theory and Its Applications*; Wiley-VCH: New York, 2000.
(83) Tolman, C. A. *Chem. Rev.* **1977**, *77*, 313–348.

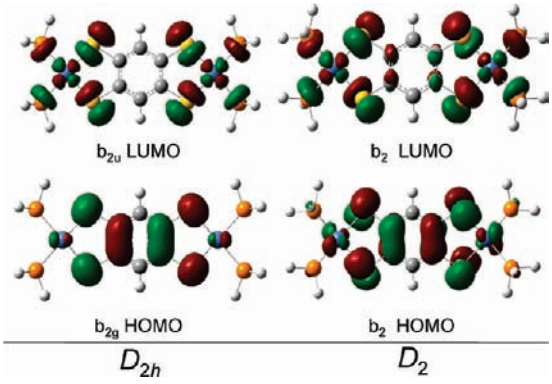

Figure 8. Composition of the HOMO and LUMO for model compound $[(PH_3)_2Ni(S_2C_6H_2S_2)Ni(PH_3)_2$ in both the D_{2h} and D_2 point groups. Contour surfaces are drawn at the 0.03 level.

consequences of ligand-field strength, model complexes were optimized with terminal trimethylphosphine ligands on Ni and Pd. Structural depictions and optimized coordinates are deposited as Supporting Information. A D_2-symmetric local minimum was located for $[(Me_3P)_2Ni(S_2C_6H_2S_2)Ni(PMe_3)_2]$. In this structure, the P−Ni−P planes are canted by 36.0° relative to the S−Ni−S planes, compared to 27.0° in the PH_3-terminated model. A similar result is obtained in the bimetallic model complex $[(Me_3P)_2Ni(S_2C_6H_2S_2)Pd(PMe_3)_2]$. Again, the palladium site is planar, but nickel adopts a geometry that is intermediate between planar and tetrahedral. Here, the S−S−P−P dihedral angle is 35.9°, compared to 26.8° in **3e′**. The corresponding dihedral angle at the palladium center is 0.95°.

The HOMO and LUMO for the $[(PH_3)_2Ni(S_2C_6H_2S_2)Ni(PH_3)_2]$ model compound are shown in both D_{2h} and D_2 point groups and are seen to have essentially the same composition in both symmetries (Figure 8). The calculations unambiguously show the HOMO to be primarily constituted of the bridging tetrathioarene ligand. Furthermore, the nature of the HOMO is antibonding with respect to the C−S bond and bonding with respect to the chelate C−C bond. Removal of an electron from this MO would shorten and lengthen, respectively, the C−S and C−C bond lengths. These changes have been observed in the crystallography of **3d** and $[\mathbf{3d}]^+$ (Table 3) and validate the use of $[(PH_3)_2Ni(S_2C_6H_2S_2)Ni(PH_3)_2]$ as a model compound to determine the essential aspects of the electronic structure of compounds **3**.

Monocation $[\mathbf{3d}]^+$ was generated in solution from **3d** by controlled potential electrolysis, and its UV−vis-near IR spectrum recorded. Figure 9 displays the absorption spectra for **3d** and $[\mathbf{3d}]^+$ for the 300−1400 nm region. The oxidation of **3d** results in the appearance of new, broad absorptions at ∼980 and 1127 nm. These spectral features contrast with the absorption spectrum of $[\mathbf{4c}]^{2+}$, which shows no absorption at energy lower than 500 nm as would be expected for a mixed-valence species. Although time-dependent DFT (TD-DFT) calculations for $[\mathbf{3d}]^+$ were not undertaken owing to the difficulties of attaining convergence with open shell systems, the qualitative appearance of the HOMO for **3d** (Figure 8) suggests that at least one of the low energy transitions for $[\mathbf{3d}]^+$ is $\pi \rightarrow \pi^*$ in nature and involves a singly occupied

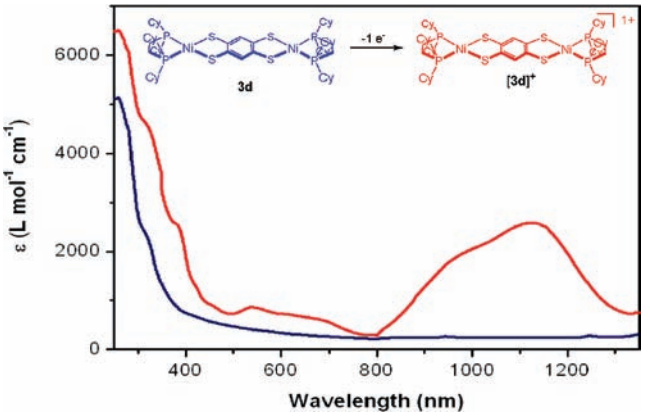

Figure 9. UV−vis near IR spectra (CH_2CI_2) for **3d** (blue) and electrogenerated $[\mathbf{3d}]^+$ (red).

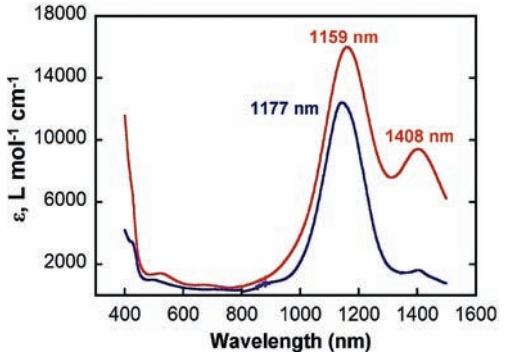

Figure 10. UV−vis and near IR spectra in DMF solution for compounds **6a** (red) and **6b** (blue).

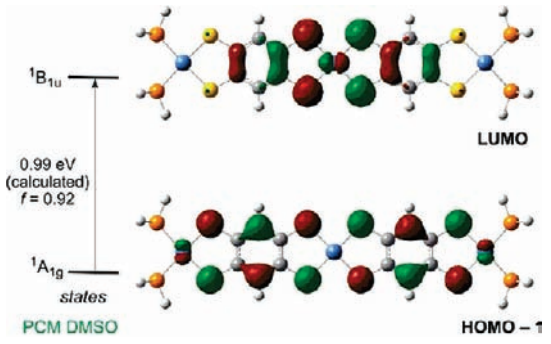

Figure 11. One of the TD-DFT calculated electronic transitions occurring in the near IR region. Contour surfaces for the model compound $[[(PH_3)_2Ni(S_2C_6H_2S_2)]_2Ni]$ are drawn at the 0.03 level.

molecular orbital (SOMO) acceptor orbital with significant admixture of sulfur p orbitals.

Compounds **6a** and **6b** also display low energy transitions in the near IR in DMF solution (Figure 10), a contrast to charge-neutral compounds **3**. These absorptions are somewhat less broad and more intense than those observed for $[\mathbf{3d}]^+$ (Figure 9). Being a closed shell compound, **6a** was amenable to TD-DFT calculations. A model compound with terminal PH_3 ligands in place of the chelating bis(phosphine) was chosen. Again, the frontier MOs are ligand-based (Figure 11). One of the allowed transitions is a HOMO-1 to LUMO excitation that is calculated to occur at 0.99 eV (~1250 nm). The LUMO acceptor orbital is π^* in nature and largely

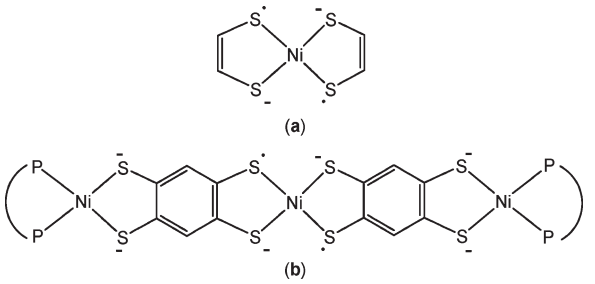

Figure 12. Analogy between mononuclear nickel bis(dithiolene) complexes, with two oxidized ligands (**a**) and **6b**, with two oxidized dithio-lene chelates (**b**). Fully reduced thiolate sulfur is represented as S^-.

composed of the central bis(dithiolene) portion of the molecule. By analogy to neutral mononuclear nickel bis(dithiolene) compounds, which have two thienyl radical monoanionic ligands with paired spins, these dithiolene ligands coordinating the center metal atom in **6a** and **6b** are where the dithiolene radical character should predominate (Figure 12). The HOMO-1 donor orbital is a π type orbital to which each of the eight sulfur atoms of the molecule appear to contribute equally, suggesting that this HOMO-1 → LUMO transition has $S^- \rightarrow S^{\bullet}$. character. Thus, the electronic absorption spectroscopy of **6a** is more closely related to $[\mathbf{3d}]^+$ than to neutral **3d**, which contains only fully reduced thiolate-type sulfur ligands.

Summary and Conclusions. Much of the synthetic work reported here involving the di- and trimetallic compounds with the tetrathioarene unit as bridging ligand hinges upon the controlled deprotection of one of two protected dithiolene chelates in a bis(dithiolene)-type ligand. Both carbonyl and di-*n*-butyl tin protecting groups have been employed, although the latter is preferred for the cleaner products that result with ensuing reactions. Trimetallic compounds **6a** and **6b** are the first bis(dithiolene)-linked trimetallic compounds produced by deliberate synthesis and structurally identified by X-ray crystallography.

The success of the synthetic methods reported here demonstrates the possibility that they can be applied another iteration for the preparation of metallodithiolene species with metal nuclearity greater than three. The known nickel bis(dithiolene) complex $[Ni(S_2C_6H_2S_2\text{-}C{=}O)_2]$[84] is a metal-expanded form of 1,3,5,7-tetrathia-*s*-indacene-2,6-dione (Scheme 1) and, in principle, subject to a controlled monodeprotection protocol. Subsequent steps analogous to those illustrated in Scheme 1 would lead to a penta-nickel product molecule that is similar to **6a** but expanded by two $[Ni(S_2C_6H_2S_2)]$ units. However, a successful extension of this chemistry may require the use of tetrathioarenes and/or chelating bis(phosphine) end groups that are functionalized with more soluble substituents. Two advantages are inherent to this method of synthesis and warrant emphasis. First, the approach is convergent in nature since separate, well-defined building blocks are taken together to produce larger, more complex assemblies. Second, the method of synthesis is such as to allow the incorporation of metals other than Ni, which may enable some degree of control over the properties of the resulting material. For example, branched structures can be imagined by the inclusion of Group 6

(84) Mizuno, M. *Synth. Met.* **1993**, *55*−*57*, 2154–2157.

metals like Mo or W, which prefer trigonal prismatic coordination geometries with dithiolene ligands.

As shown in our crystallographic studies, the tetrathioarene-linked di- and trimetallic compounds are not strictly rigid but instead able to tolerate appreciable distortions from planarity. Compounds **3d** and **3e** show modest end-to-end folding in the crystalline state, which is attributed to crystal packing effects, while trimetallic compounds **6a** and **6b** reveal a surprising degree of twisting (20°) and end-to-end bending (46°), which shows they are by no means rigid, rod-like molecules but more like flexible dumbbells. These deformation types observed in the crystalline state are undoubtedly sampled to some extent in solution as well and are a consideration to bear in mind in understanding their solution spectra.

Our collective electrochemical data for compounds **2a**-**2d** and **3a**-**3d** are consistent and clear in pointing toward the tetrathioarene unit as the redox active entity within these molecules. Key observations include the sensitivity of compounds **3** toward the PF_6^- electrolyte anion when cyclic voltammetry in the anodic direction is performed and, in contrast, the well-behaved reversible behavior observed when an electrolyte with the weakly coordinating $BArF_{24}^-$ anion is employed. To the best of our knowledge, previous transition metal systems involving the use of the 1,2,4,5-benzenetetrathiolate bridging ligand have not displayed redox processes that were attributed to the tetrathioarene unit. Clearly, the work presented here emphasizes that the possibility for ligand-based redox chemistry in any tetrathioarene-bridged dimetal system must be carefully examined.

The foregoing interpretation regarding ligand redox noninnocence in compounds **3** is confirmed by structural data for [**3d**$^+$] and by the DFT-calculated electronic structure of a model for compounds **3**, which reveals the HOMO to be constituted primarily of the bridging $S_2C_6H_2S_2$ ligand. Another, very useful diagnostic for distinguishing metal-based versus ligand-based mixed valency in oxidized forms of these tetrathioarene compounds is near IR spectroscopy, which is an energy region in which transition(s) are operative to a low-lying π^* acceptor orbital containing an unpaired spin delocalized throughout the tetrathiobenzene bridging ligand.

Continuing work by our groups will extend these exploratory syntheses and physical studies to more complex, higher nuclearity metallodithiolene systems.

Acknowledgment. The Petroleum Research Fund is thanked for support to J.P.D. (Grant 45685-G3) and T.G.G. (Grant 42312-G3). Support from the National Science Foundation (Grant CHE-0749086 to T.G.G.; Grant CHE-0845829 to J.P.D.) is gratefully acknowledged. T.G.G. is an Alfred Sloan Foundation Fellow. The Louisiana Board of Regent is thanked for the support with which Tulane University's CCD diffractometer was obtained (Grant LEQSF-(2002-03)-ENH-TR-67), and Tulane University is thanked for its ongoing support of the X-ray diffraction laboratory. Prof. Daniel G. Nocera is thanked for access to a near IR spectrophotometer. Prof. Bill Geiger of the University of Vermont is thanked for helpful discussion regarding aspects of the electrochemical studies reported here.

Supporting Information Available: Details pertaining to crystal growth, X-ray diffraction data collection, structure solution and refinement; selected structural parameters for all compounds (Tables S1−S6); full crystallographic details for all structurally characterized compounds in CIF format; thermal ellipsoid plots of all compounds with full atomic labeling; computational details; atomic coordinates for all geometry optimized model compounds (Tables S7−S12). This material is available free of charge via the Internet at http://pubs.acs.org.